

Advanced Liquid Electrolyte Design for High-Voltage and High-Safety Lithium Metal Batteries

Junhua Zhou, Huimin Wang, Yongqiang Yang, Xinyan Li, Can Guo, Zhibo Li, Shujing Wen, Jiehua Cai, Zhaokun Wang, Yufei Zhang, Qiyao Huang, and Zijian Zheng*

High-voltage lithium metal batteries (LMBs) represent a promising technology for next-generation energy storage, yet their commercialization is impeded by rapid performance degradation and safety concerns. Key challenges include lithium dendrite growth, unstable solid electrolyte interphase (SEI) and cathode electrolyte interphase (CEI), aluminum current collector corrosion, electrolyte oxidative decomposition, and inherent electrolyte flammability. This review systematically discusses strategies to overcome these issues by designing advanced liquid electrolytes, including: 1) regulating Li⁺ solvation structures via highly concentrated electrolytes (HCEs) or localized HCEs to stabilize Li deposition and suppress dendrites; 2) designing weakly solvating electrolytes with tailored solvent molecules to enhance SEI/CEI robustness; 3) leveraging ionic liquids as nonflammable solvents with high electrochemical stability to mitigate electrolyte oxidation and Al corrosion; and 4) incorporating flame-retardant phosphorus- or chlorine-based solvents to improve electrolyte safety. Perspectives on future research directions emphasize developing advanced in situ and full-cell-based characterization techniques, optimizing interfacial engineering, and scaling up cost-effective electrolyte formulations, to accelerate the practical development of high-voltage, high-safety LMBs for the next-generation energy storage.

1. Introduction

Lithium metal batteries (LMBs) represent a promising energy storage technology for meeting the growing demands of electric vehicles, renewable energy grids, and advanced portable electronics.[1-3] Lithium (Li) metal anodes offer an ultrahigh theoretical capacity of 3860 mAh g-1 and the lowest electrochemical potential (-3.04 V vs standard hydrogen electrode), enabling LMBs to achieve specific energy exceeding 500 Wh kg⁻¹, nearly double that of conventional lithium-ion batteries (LIBs) using the graphite anode with theoretical capacity of only 375 mAh g⁻¹ (**Figure 1a**).^[4-6] However, LMBs face critical challenges including Li metal dendrite growth, electrolyte instability at high voltages (>4.3 V vs Li/Li⁺), and safety concerns such as thermal runaway. $[\dot{7}-10]$ These issues are deeply interconnected: dendritic growth accelerates electrolyte depletion and internal short-circuit risks; cathode oxidation triggers transition metal dissolution, degrading both electrodes; and flammable organic solvents exacerbate fire hazards under thermal/mechanical abuse.[2,9]

Multiple approaches have been developed to address these challenges.

Solid-state electrolytes (SSEs) eliminate flammability and physically block dendrites but suffer from poor interfacial contact, low room-temperature ionic conductivity, and manufacturing scalability barriers.^[11,12] Anode engineering via 3D conductive hosts or artificial SEI layers mitigates dendrite propagation but

J. Zhou, H. Wang, Y. Yang, X. Li, C. Guo, Z. Li, S. Wen, Z. Wang, Y. Zhang, 7 Zheng

Department of Applied Biology and Chemical Technology The Hong Kong Polytechnic University

Hong Kong SAR 999077, China E-mail: tczzheng@polyu.edu.hk

J. Cai, Q. Huang, Z. Zheng School of Fashion and Textiles The Hong Kong Polytechnic University Hong Kong SAR 999077, China

The ORCID identification number(s) for the author(s) of this article can be found under https://doi.org/10.1002/aenm.202502654

© 2025 The Author(s). Advanced Energy Materials published by Wiley-VCH GmbH. This is an open access article under the terms of the Creative Commons Attribution License, which permits use, distribution and reproduction in any medium, provided the original work is properly cited

DOI: 10.1002/aenm.202502654

Q. Huang, Z. Zheng Research Institute for Intelligent Wearable Systems The Hong Kong Polytechnic University Hong Kong SAR 999077, China

Z. Zheng Research Ins

Research Institute for Smart Energy The Hong Kong Polytechnic University Hong Kong SAR 999077, China

Z. Zheng

PolyU-Daya Bay Technology and Innovation Research Institute Huizhou 516083, China

Z. Zheng

PolyU-Wenzhou Technology and Innovation Research Institute Wenzhou 325024. China

16/14684, 2023, 34. Downloaded from https://advanced.onlinelibrary.wiley.com/doi/10.1002/mem.20230254 by HONG KONG POLYTECHNIC UNIVERSITY HU NG HOM, Wiley Online Library on [25/09/2025]. See the Terms and Conditions (https://onlinelibrary.wiley.com/terms-and-conditions) on Wiley Online Library for rules of use, OA articles are governed by the applicable Centwive Commons Licenses

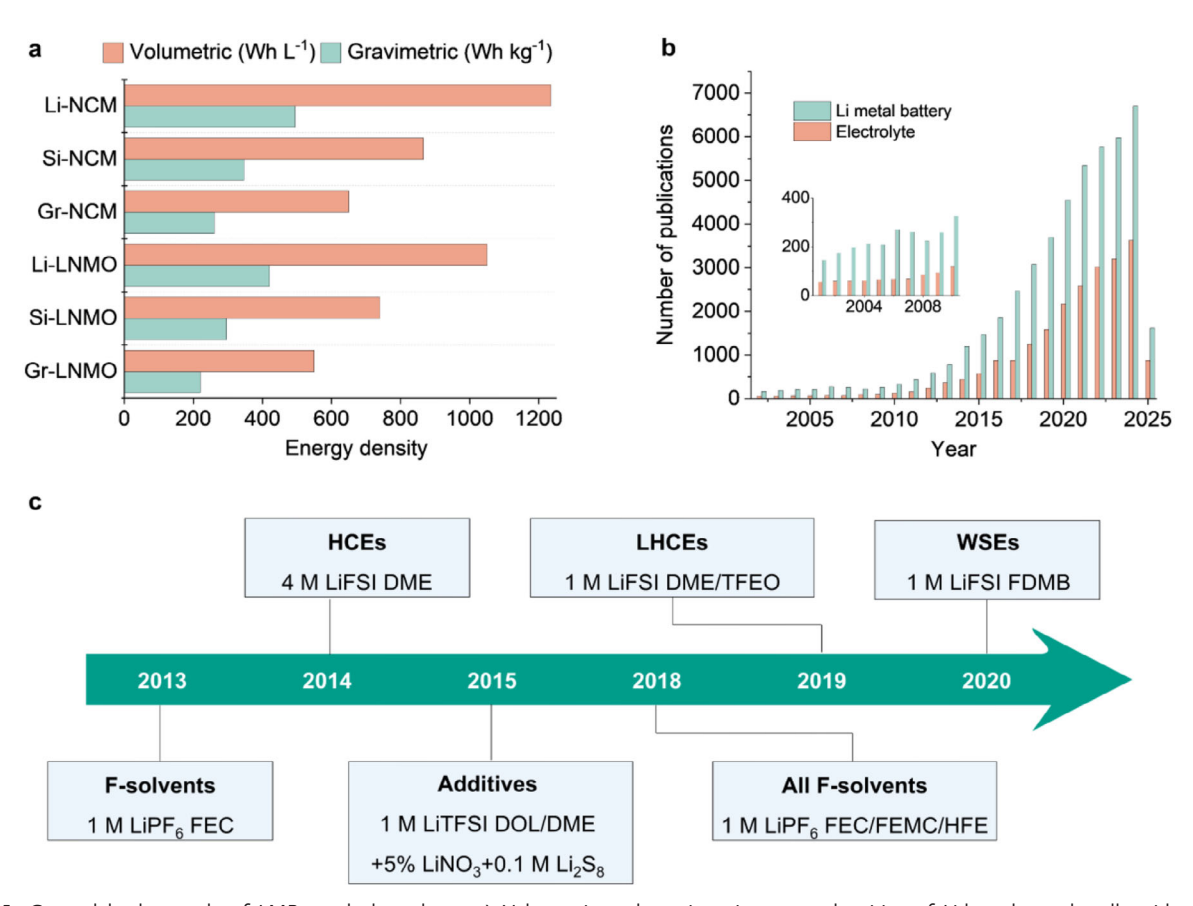


Figure 1. General backgrounds of LMBs and electrolytes. a) Volumetric and gravimetric energy densities of Li-based pouch cells with different anode–cathode pairs, including Li metal, Si, and graphite (Gr) anodes, $LiNi_xCo_yMn_{1-x-y}O_2$ (NCM), and $LiNi_{0.5}Mn_{1.5}O_4$ (LNMO). Reproduced with permission. [4] Copyright 2024, Wiley-VCH. b) Number of publications associated with LMBs and electrolytes since 2000. The presented values are obtained from Web of Science via keywords search: "Li metal battery" or "electrolyte." c) A historical outline of the development of liquid electrolytes for LMBs. The timeline shows the key developments: high-concentration electrolytes (HCEs), such as 4 M lithium bis (fluorosulfonyl) imide (LiFSI) in 1,2-dimethoxyethane (DME); localized high-concentration electrolytes (LHCEs), such as 1 M LiFSI in DME and tris (2,2,2-trifluoroethyl) orthoformate (TFEO); weakly solvating electrolytes (WSEs), such as 1 M LiFSI in fluorinated 3,4-dimethoxylbutane (FDMB); electrolytes with fluorinated solvents (F-solvents), such as 1 M LiFF₆ in fluoroethylene carbonate (FEC); electrolytes with functional additives, such as 1 M lithium bis (trifluoromethanesulphonyl) imide (LiTFSI) in DME and 1,3-dioxolan (DOL) with lithium polysulfide (e.g., Li_2S_8) and $LiNO_3$ additives; all-fluorinated electrolytes, such as 1 M LiPF₆ in FEC, 3,3,3-fluoroethylmethyl carbonate (FEMC), and 1,1,2,2-tetrafluoroethyl-2,2,3,3-tetrafluoropropyl ether (HFE).

introduces cost and energy density trade-offs. [13] Cathode surface coatings (e.g., Al_2O_3 , Li_3PO_4) and structural doping (e.g., Al, Mg, Ti) enhance high-voltage stability yet cannot fully prevent electrolyte decomposition. [14] System-level protections like advanced battery management systems detect failures reactively but do not resolve underlying electrochemical instabilities. By contrast, advanced liquid electrolytes remain a pivotal near-term solution due to their compatibility with existing manufacturing infrastructure, tunable interphase chemistry, and superior charge-transfer kinetics. By integrating multifunctional solvents, stable salts, and optimized solvation structures, next-generation liquid electrolytes can synergize with electrode and system innovations to holistically address LMB challenges, enabling a viable pathway toward high-energy-density, safe, and durable batteries.

However, developing high-voltage LMBs in liquid electrolyte is still very challenging. Commercial ethylene-carbonate (EC)-based electrolytes demonstrate desirable performance in LIBs because they can form stable organic-inorganic hybrid solid-

electrolyte interphases (SEIs) that prevent graphite exfoliation at the anode, and maintain electrochemical stability up to 4.2 V, making them compatible with conventional cathodes such as LiFePO₄ and NCM811.^[15] However, in LMBs, the high reactivity and significant volume expansion of Li metal anodes during plating/stripping rupture the fragile SEI, triggering continuous parasitic reactions and low Coulombic efficiency (CE < 90%).^[16–18] Furthermore, under high voltages (>4.3 V), EC-based electrolytes oxidize at the cathode, which accelerates transition metal (TM) dissolution and structural degradation, thereby limiting high-energy-density designs.^[14] Last but not the least, their inherent volatility and flammability pose severe safety risks under mechanical/thermal abuse,^[19,20] while Li dendrite growth exacerbates internal short-circuit hazards.^[21,22]

Research interests in LMBs and electrolytes have been increasing sharply since 2015 based on the number of publications on Web of Science (Figure 1b), and numerous advanced electrolyte designs have been developed to improve the CE of Li metal anodes (Figure 1c). [23,24] The CE values of Li metal



www.advenergymat.de

anodes referenced in this review were all measured in Li-Cu half-cells, as this configuration isolates anode-specific performance. Half-cell CE provides a benchmark for SEI quality, critical for assessing practical viability. The success of reported electrolytes is to form inorganic-rich interphases (LiF is the most preferred), which endow high interfacial energy toward Li metal anodes to suppress dendrite growth, and high mechanical strength to inhibit SEI rupture. [25,26] Early efforts focused on optimizing carbonate solvents, where the fluoroethylene carbonate (FEC) was found to generate more uniform and LiFrich SEI than other carbonates, including EC, propylene carbonate (PC), dimethyl carbonate (DMC), and ethyl methyl carbonate (EMC). This approach achieved a notable CE of 98.2% in 1 M LiPF₆/FEC electrolytes.^[27] Inspired by this idea, allfluorinated strategy was subsequently designed via applying FEC, 3,3,3-fluoroethylmethyl carbonate (FEMC), and 1,1,2,2tetrafluoroethyl-2,2,3,3-tetrafluoropropyl ether (HFE) as cosolvents. The resulting electrolyte (1 M LiPF₆ in FEC/FEMC/HFE) demonstrated exceptional compatibility with high-voltage cathodes (e.g., 5 V level LiCoPO₄), while maintaining 99.2% CE of Li metal anodes. [28,29] Beyond solvent fluorination, regulating the concentration of Li salts is another effective strategy. For example, HCEs (e.g., 4 m lithium bis(fluorosulfonyl)imide (LiFSI) in 1,2-dimethoxyethane (DME)), could minimize free solvent molecules, facilitate an anion-derived LiF-rich SEI, and consequently achieve 99.1% CE.[30] However, HCEs suffer from high viscosity, which compromises Li+ conductivity and rate capability. To mitigate this, localized high-concentration electrolytes (LHCEs) were developed by diluting HCEs with nonsolvating fluorinated solvents (e.g., tris(2,2,2-trifluoroethyl) orthoformate (TFEO)).[31] For instance, 1 M LiFSI in DME/TFEO formed a monolithic, amorphous F-rich SEI, enabling 99.5% CE by minimizing Li pulverization and high Li⁺ conductivity. Despite these advances, the presence of strong-solvating solvents (e.g., DME) in HCEs/LHCEs often leads to low initial CE due to excessive Li metal consumption.[32,33] This limitation inspired the design of weakly solvating fluorinated solvents (e.g., fluorinated 1,4dimethoxylbutane (FDMB)), enabling single-solvent, single-salt electrolytes (1 M LiFSI/FDMB).[34] As a weakly solvating electrolyte (WSE), this system features anion-dominated solvation structures, ultrathin (≈6 nm) SEIs, and remarkable compatibility with both Li metal anodes (99.52% CE) and high-voltage cathodes (>6 V stability). Additive engineering also advanced the field, such as lithium polysulfide (e.g., Li₂S₈) and LiNO₃, which synergistically create a robust inorganic SEI that mitigated electrolyte decomposition and enable dendrite-free cycling of Li metal with 99.1% CE.[35,36] LiNO₃ is widely used to promote Li₂N/LiN_xO_yrich SEI on Li metal anodes, but it exhibits severe incompatibilities with high-Ni cathodes. Similarly, while polysulfides promote Li2S/Li2SO2-rich SEI on Li anodes, they trigger aggressive degradation at high-Ni cathodes. Therefore, the concentrations of these additives in electrolytes for high-voltage LMBs are normally controlled less than 0.5 M to eliminate the parasitic

Despite these advancements in improving Li metal anode cyclability, critical gaps remain in understanding electrolyte stability under high-voltage conditions and ensuring safety. High-voltage tolerance depends on oxidative resistance of Li salts and solvents, Al current collector corrosion induced by Li salts, and

the properties of the cathode electrolyte interphase (CEI). [37,38] However, research on the CEI remains in its infancy. Unlike Li metal anodes, high-voltage cathodes feature complex architectures comprising active materials, conductive additives, and binders. The complexity of cathode components complicates the compositional analysis of CEI. Furthermore, CEI exhibits inferior stability and lower abundance compared to SEI due to more aggressive oxidative reactions at high voltages. A further challenge lies in designing electrolytes that simultaneously achieve high performance and intrinsic safety. Current safety assessments primarily focus on electrolyte flammability rather than full-cell evaluations, which fail to accurately reflect real-world LMB behavior.

While solid-state electrolytes offer potential safety advantages for LMBs, their commercialization remains hindered by manufacturing scalability challenges. This review consequently focuses on advanced liquid electrolyte strategies for developing high-voltage, high-safety LMBs. Three fundamental challenges will be discussed first, including electrolyte depletion, unstable SEI, and dendrite growth toward Li metal anodes, electrolyte oxidation, unstable CEI, and Al corrosion toward high-voltage cathodes, and safety concerns about dendritic Li metals and flammable electrolytes. The corresponding strategies cover regulating concentration of Li salts to prepare HCEs and LHCEs, designing structure of solvent molecules to prepare WSEs, applying highly stable ionic liquids (ILs), or flame-retardant phosphorus (P)-/chlorine (Cl)-based molecules as electrolyte solvents. Conclusions and perspectives will be finally proposed to guide further research directions to promote practical high-voltage and high-safety LMBs better. This review establishes a distinct viewpoint by systematically addressing the critical synergy between achieving high-voltage operation (>4.5 V) and intrinsic safety, a dual challenge often treated separately in previous literature but essential for practical LMBs.

2. Challenges of Developing High-Voltage and High-Safety Liquid Electrolytes

The development of high-voltage, safe liquid electrolytes for LMBs faces three interconnected fundamental challenges: 1) inherent safety hazards from flammable organic solvents and reactive Li metal; 2) thermodynamic instability at Li metal anodes causing dendrite growth, unstable SEI, and electrolyte depletion; and 3) electrochemical incompatibility with high-voltage cathodes, leading to oxidative decomposition, unstable CEI, and Al current collector corrosion. These challenges stem from conflicting physicochemical requirements, ionic conductivity versus electrochemical stability, interfacial passivation versus Li⁺ transport kinetics, and energy density versus safety, which must be balanced to enable practical high-energy-density LMBs.

2.1. Safety Concerns about Flammable Electrolytes and Dendritic Li Metals

The commercialization of LMBs faces significant safety barriers, particularly concerning thermal runaway events that can

16146840, 2025, 34, Downloaded from https://advanced.onlinelibrar;

10.1002/aenm 2025/02654 by HONG KONG POLYTECHNIC UNIVERSITY HU NG HOM, Wiley Online Library on [25/09/2025]. See the Terms and Conditions

nline library wiley.com/terms-and-conditions) on Wiley Online Library for rules of use; OA articles are governed by the applicable Creative Commons

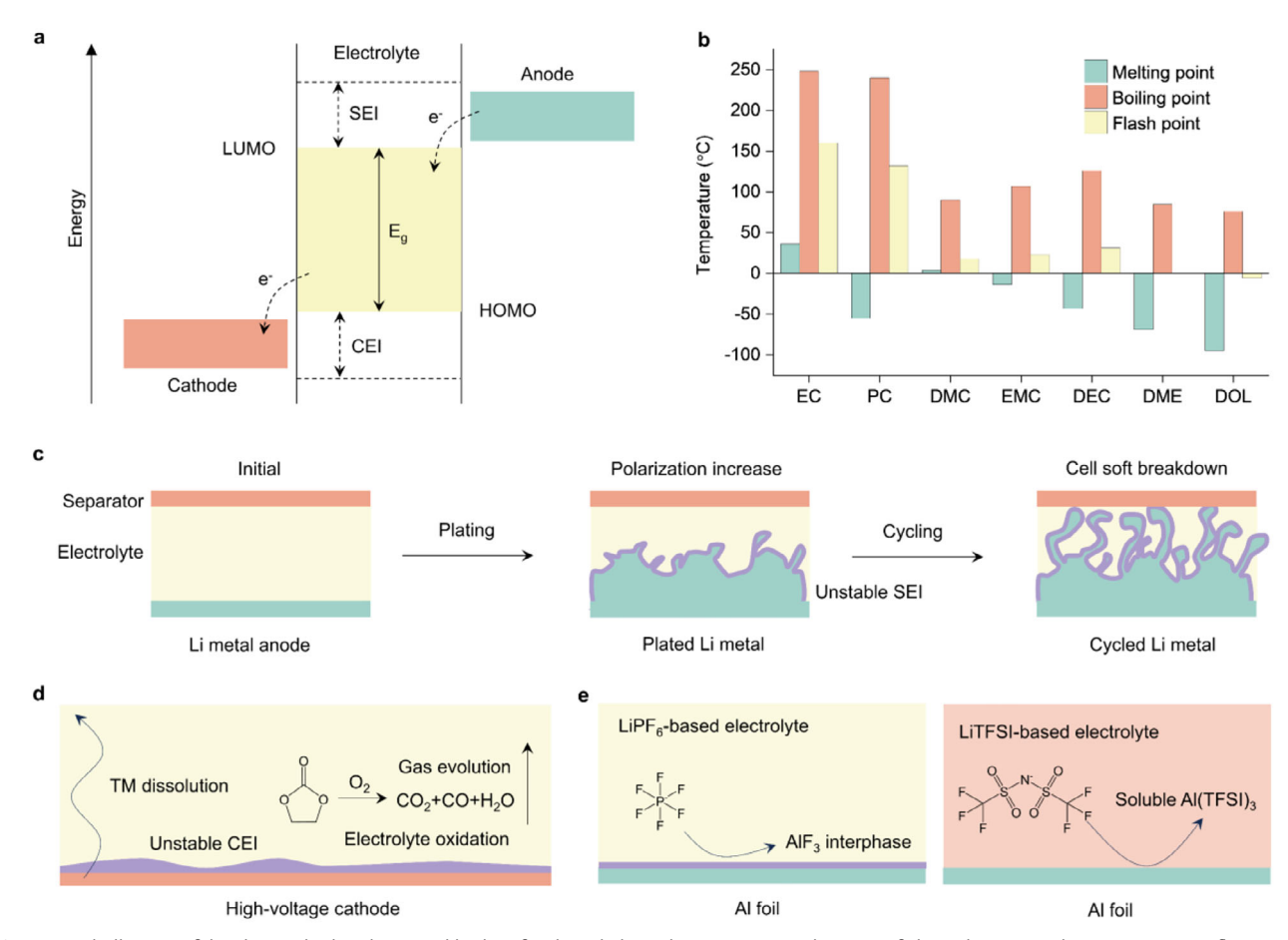


Figure 2. Challenges of developing high-voltage and high-safety liquid electrolytes. a) Energy diagram of electrolytes. Four key parameters influence the electrochemical window of electrolytes, including the lowest unoccupied molecular orbital (LUMO), highest occupied molecular orbital (HOMO), SEI, and CEI. b) Melting points, boiling points, and flash points of common electrolyte solvents: EC, PC, DMC, EMC, diethyl carbonate (DEC), DME, and DOL. c) Challenges during Li stripping/plating process, including the polarization increase and cell soft breakdown. d,e) Challenges of high-voltage cathodes with conventional organic liquid electrolytes, including (d) interphase cracking, electrolyte decomposition, TM dissolution, and (e) Al current collector corrosion.

lead to fires or explosions. These hazards originate from the extreme reactivity of Li metal anodes and the inherent flammability of conventional electrolytes. The primary driver of Li metal reactivity is its inherent thermodynamic instability in conventional electrolytes. Li metal possesses the lowest electrochemical potential among all elements. This results in a Fermi level significantly higher than the lowest unoccupied molecular orbital (LUMO) energy level of most organic electrolytes. The large energy gap between Li's Fermi level and the electrolyte's LUMO drives spontaneous electron transfer from Li to electrolyte molecules, triggering reductive decomposition (Figure 2a). [39] The high diffusivity of Li⁺ ions and low energy barriers for surface diffusion enable rapid Li deposition at defects. This kinetic preference, combined with thermodynamic instability, creates a self-accelerating reaction. Upon contact with electrolytes, Li spontaneously forms unstable SEI with inherent inhomogeneity. This irregular SEI structure promotes uneven Li deposition during cycling, leading to dangerous dendrite formation.[40]

Under thermal/mechanical abuse, electrolyte solvents with low flash points (<40 $^{\circ}\text{C},$ Figure 2b) vaporize and decompose

into flammable gases, including C2H4 (from EC reduction), H2 (from Li-H2O reactions), CO (from carbonate oxidation), and light hydrocarbons (e.g., CH₄, C₂H₆). These gases form explosive mixtures with atmospheric oxygen, such as H_2 (4–75 vol%), C_2H_4 (3.0–34 vol%), and CO (12.5–74 vol%), which ignite upon contact with sparks or hot surfaces. Ether solvents (e.g., DME, 1,3-dioxolan (DOL)) further risk peroxide formation, which decomposes explosively. Thermal runaway initiates when localized temperatures exceed the autoignition threshold of solvents (e.g., DMC: 18 °C), driven by Arrhenius-type decomposition kinetics: $RH \xrightarrow{k_1} R \cdot + H \cdot (k_1 = Ae^{-E_a/RT})$, where $E_a = 150-200 \text{ kJ mol}^{-1}$ for C-H bond cleavage in carbonates. Radical chain reactions (H · $+O_2 \rightarrow HO \cdot +O \cdot$) release large amounts of heat, while dendritic Li amplifies combustion by increasing reactive surface area. Concurrently, Joule heating at dendrite tips using the power dissipation model: $P = I^2 R_{\rm shot} = \frac{V^2}{R_{\rm short}}$, where $R_{\rm short}$ (dendrite resistance) = 10–100 Ω , generating localized high temperatures within milliseconds. Sequential reactions amplify heat generation, including SEI decomposition (80-120 °C), electrolyte combustion (120-200 °C), and cathode decomposition (>200 °C). These





www.advenergymat.de

exothermic processes cause cell rupture, fire, or explosion, with risk of propagation in battery packs.^[10,41]

2.2. Electrolyte Depletion, Unstable SEI, and Dendrite Growth toward Li Metal Anodes

The fundamental challenge of Li metal anodes lies in their inherent thermodynamic instability in conventional liquid electrolytes, which leads to uncontrolled dendritic growth (Figure 2c). [42,43] During electrodeposition, the reduction of Li⁺ ions preferentially occurs at inhomogeneous nucleation sites rather than forming uniform layers, driven by localized electric field and nonuniform ion flux distributions.[44,45] Dendrite nucleation is governed by Sand's time $(\tau = \frac{\pi D}{4} (\frac{eC_0 \mu}{J})^2)$, where $D = \text{Li}^+$ diffusion coefficient, C_0 = bulk concentration, μ = cation transference number, and J= current density. Low μ (<0.3 in carbonates) and high J (>1 mA cm⁻²) shorten τ , promoting nonuniform deposition. [46] Dendrite nucleation can be further analyzed using Gibbs free energy calculation: $\Delta G = -\frac{zF\eta}{r} \cdot V_{\rm m} + \gamma A$, where η = overpotential, $V_{\rm m}$ = molar volume of Li, and γ = surface energy. Low γ sites (e.g., grain boundaries, defects) favor heterogeneous nucleation at η > 20 mV. Density functional theory (DFT) calculations show Li adsorption energy varies by >0.5 eV across SEI components, driving preferential deposition. This results in the formation of high-surface-area dendritic morphologies, ranging from needlelike protrusions to mossy structures, that readily penetrate electrolytes and separators.[13,47] Li's unique surface diffusion characteristics and lack of host matrices further exacerbate this dendritic growth tendency.[48,49]

The inherent fragility and compositional heterogeneity of SEI moreover present challenges for Li metal anodes. This passivation layer, formed through electrolyte reduction at the Li surface, consists of an irregular mosaic of inorganic (LiF, Li2O, Li3N) and organic components (e.g., alkyl carbonates) with varying mechanical and transport properties.[50,51] The SEI's nonuniform ionic conductivity creates localized ion transport that concentrates Li⁺ flux at specific sites, promoting dendritic nucleation.^[52] Moreover, the SEI's brittle structure cannot accommodate the significant volume changes during Li plating/stripping, which leads to mechanical fracture after cycling. SEI fracture mechanics are described using strain-energy release rate (*G*): $G = \frac{\sigma^2 \pi a}{\sigma}$, where $\sigma = \text{stress during Li plating (up to 1 GPa)}, a = \text{SEI}$ crack size, and E = 50-100 GPa (Young's modulus). Organic-rich SEI (E < 10 GPa) fractures at a > 10 nm, exposing fresh Li to electrolytes.[26] This continuous SEI breakdown exposes fresh Li to the electrolyte, driving parasitic reactions that deplete both active Li and electrolyte. [53,54] The resulting accumulation of electrically isolated "dead Li," which consists of fractured Li fragments that lose contact with current collectors, causing irreversible capacity loss and CE degradation.[55,56]

2.3. Electrolyte Oxidation, Unstable CEI, and Al Corrosion toward High-Voltage Cathodes

Electrolyte oxidative stability fundamentally hinges on the energy alignment between the solvent's highest occupied molecular orbital (HOMO) energy level and the cathode's Fermi level un-

der high-voltage operation (>4.3 V vs Li/Li⁺). Conventional carbonate solvents (e.g., EC: -7.21 eV; DMC: -7.05 eV) exhibit insufficient oxidation resistance due to their electron-rich oxygen atoms, which lower the activation barrier ($E_{\rm a}$) for dehydrogenation and ring-opening reactions at charged cathodes. [8,14] For instance, EC decomposition initiates via hydrogen abstraction at α -carbons, generating CO₂, ethylene gas, and radical intermediates that propagate electrolyte oxidation (Figure 2d). This process is dramatically accelerated by TM catalysis. Dissolved Ni³⁺/Mn³⁺ from layered or spinel cathodes reduces $E_{\rm a}$ by facilitating electron transfer from solvents to lattice oxygen, triggering TM dissolution and oxygen release. Concurrently, LiPF₆ hydrolysis produces HF, which etches cathode surfaces, exacerbating TM dissolution and forming resistive Li_xPO_yF_z phases that increase impedance. [9]

The CEI formed at high-voltage cathodes (>4.3 V) exhibits limitations that compromise battery performance. Unlike its anode counterpart (SEI), the CEI develops through uncontrolled electrolyte decomposition under extreme oxidative conditions, resulting in a structurally fragile and chemically heterogeneous passivation layer.[57] This inherent instability exhibits failure modes, including nonuniform ion transport that creates localized hotspots that accelerate electrolyte oxidation and TM dissolution, dissolved TM ions migrate to the anode where they catalyze SEI degradation and promote irregular Li deposition, and continuous CEI fracture during cycling. These evolutions finally lead to cathode phase transitions, oxygen release, and electrolyte depletion.^[58,59] The CEI's stability critically depends on its composition, where LiF plays significant roles. Its wide electrochemical stability (>6 V) suppresses oxidative decomposition at high voltages.

The corrosion of Al current collectors at high voltage remains a barrier to adopting advanced Li salts such as LiFSI and lithium bis(trifluoromethanesulphonyl)imide (LiTFSI). Conventional LiPF₆-based electrolytes enable stable AlF₃-rich passivation layers that protect Al foil up to 4.3 V. LiFSI and LiTFSI, despite their superior thermal stability and oxidation resistance, trigger severe Al dissolution at potentials above 4.2 V (Figure 2e). [60] This corrosion mechanism stems from the electrochemical oxidation of FSI⁻ or TFSI⁻ anions, which react with Al foil to form soluble complexes (e.g., Al(FSI)₃, Al(TFSI)₃) rather than the protective AlF₃ layer. The resulting continuous dissolution exposes fresh Al surfaces, accelerating corrosion and increasing interfacial resistance. Under high-voltage cycling conditions (>4.5 V), this degradation pathway becomes particularly severe, which leads to rapid capacity fade, voltage decay, and safety risks from localized current collector thinning.[61,62]

3. Strategies of Developing High-Voltage and High-Safety Liquid Electrolytes

The design of high-voltage and high-safety electrolytes for LMBs depends on addressing critical challenges: stabilizing Li metal anodes to suppress dendrites, preventing oxidative decomposition at high-voltage cathodes, and mitigating flammability risks. Addressing these challenges demands electrolytes with precisely tuned properties. First, ion transport properties, including ionic conductivity, Li⁺ transference number (t_{Li}^+), and viscosity, are discussed in relation to rate capability and polarization. While



ADVANCED ENERGY MATERIALS

www.advenergymat.de

high ionic conductivity (>10 mS cm $^{-1}$) is essential for minimizing ohmic losses, a high $t_{\rm Li}^+$ (>0.4) is even more critical to reduce concentration gradients that accelerate dendrite growth. This is quantitatively linked to Sand's time, where low $t_{\rm Li}^+$ values promote dendritic failure. Second, HOMO–LUMO energies could be used to predict oxidative/reductive limits of solvents/salts. Key metrics include the electrochemical stability window (>4.5 V for high-voltage cathodes) and the role of solvation structures in shifting reduction potentials. Third, thermal stability is addressed via flash points, self-extinguishing time (SET), and decomposition pathways (e.g., LiPF $_6$ hydrolysis to HF above 60 °C).

In this review, HCEs/LHCEs leverage elevated Li salt concentrations to shift Li+ solvation from solvent-dominated to anionrich coordination, promoting inorganic-rich SEIs and CEIs that enhance Li metal anode and high-voltage cathode stability. Meanwhile, HCEs and LHCEs improve LMBs' safety by reducing free solvent molecules, which minimizes electrolyte flammability and suppresses parasitic reactions. WSEs, designed with solvents exhibiting low donor numbers, weaken Li+-solvent binding, which promotes preferential anion reduction, fostering robust SEIs and CEIs. Simultaneously, WSEs enhance the safety of LMBs by incorporating nonflammable solvents such as fluorinated solvents, lowering electrolyte volatility and flammability. ILs, inherently nonflammable and thermally stable, offer ultrawide electrochemical windows (>5 V) due to their high anodic stability, making them ideal for high-voltage and high-safety systems. Flameretardant P- or Cl-based solvents chemically interrupt combustion chains through radical scavenging, which improve safety of LMBs greatly. By engineering solvation structures to favor inorganic interphases and integrating flame-retardant chemistries, these approaches overcome the traditional trade-offs between energy density and safety, paving the way for practical high-voltage LMBs capable of meeting the demands of next-generation energy storage.

3.1. Regulating Concentration of Li Salts to Prepare HCEs and LHCEs

The electrolyte's solvation structure fundamentally governs its electrochemical performance. In conventional low-concentration electrolytes (LCEs, ≈1 M), Li⁺ ions primarily coordinate with solvent molecules, forming a solvent-dominated solvation structure (Figure 3a,b).[9,63] Under electric field, Li⁺ ions carry solvent molecules into electric double layer close to Li metal, where the solvents decompose and form organic-rich SEI.^[64] Such SEI exhibits low mechanical strength and fails to withstand the stress caused by Li dendrite growth, leading to continuous SEI fracture and reformation. When HCEs are employed by increasing the concentration of Li salts to more than 4 M, Li⁺ ions instead coordinate predominantly with anions, creating an anion-dominated solvation structure. [65] This facilitates the formation of inorganicrich SEI and CEI, endowing desirable compatibility with both Li metal anodes and high-voltage cathodes. However, HCEs face challenges such as increased viscosity and reduced ionic conductivity, impairing fast-charging capabilities. [66] To address these issues, LHCEs prepared by introducing nonsolvating diluents into HCEs can reduce the salt concentration to around 1 m, while maintain the anion-dominated solvation structure. [67]

While both HCEs and LHCEs leverage concentrated Li+-anion clusters to stabilize interfaces, their structural and functional differences are profound. HCEs (e.g., 4 M LiFSI/DME) create a percolating network of contact ion pairs and aggregates, eliminating free solvents and enabling uniform anion-derived SEI/CEI formation. However, their high viscosity (>30 mPa s) and low conductivity (<2 mS cm⁻¹) limit rate capability and practical viability. LHCEs (e.g., 1 M LiFSI/DME/TTEO) strategically dilute HCEs with nonsolvating agents that preserve localized high-concentration clusters while reducing global salt content. This design lowers viscosity by 50-70% and increases conductivity to >4 mS cm $^{-1}$, enabling fast charging (3–5 C) and compatibility with industrial electrode loadings. [67] Crucially, LHCEs retain interfacial advantages by confining anion decomposition to nanoscale domains and reducing parasitic reactions through diluent-mediated solvent exclusion.

The precise solvation structure of HCEs and LHCEs could be regulated by kinds of Li salts, solvents, and diluents (Figure 3b). Currently, the reported Li salts primarily include LiPF₆, [68] LiBF₄, [69,70] lithium bis(oxalato)borate (LiBOB), [71] lithium difluoro(oxalato)borate (LiDFOB),[72] LiFSI,[73] LiTFSI,[74] and LiNO₃.^[75] Salt choice critically dictates HCE/LHCE functionality. LiFSI's dominance stems from its unparalleled solubility and LiF-forming ability, but its tendency to corrode Al above 4.2 V requires mitigation strategies such as fluorinated diluents or hybrid salt systems. LiTFSI, while thermally robust, exacerbates corrosion and increases viscosity, making it less suitable for high-power applications. Industrially prevalent LiPF₆ offers Al compatibility but decomposes above 4.3 V and hydrolyzes to HF, limiting high-voltage viability. Emerging salts like LiDFOB enable stable cycling at extreme voltages (e.g., 4.8 V LiNi_{0.5}Mn_{1.5}O₄ (LNMO)) through boron–fluoride hybrid interphases but face solubility constraints. Thus, salt selection involves balancing interphase quality, voltage tolerance, and kinetic performance.[9]

Typical solvents include DMC,^[76] PC,^[77] FEC,^[78,79] FEMC,^[80] DME,^[81] ethylene glycol diethyl ether (DEE),^[82] sulfolane (SL),^[83,84] and triethyl phosphate (TEP).^[75] The average CEs of Li metal anodes show differences depending on the coordinating solvent selected, which follow the order as: 99.1% (TEP—LHCE) < 99.2% (TMS—LHCE) < 99.3% (DMC—LHCE) < 99.5% (DME—LHCE),^[85] In DME—LHCE, weak LiFSI—DME coordination promotes preferential salt reduction, forming a robust, inorganic-rich SEI (high LiF/Li₃N content) that minimizes parasitic reactions and Li loss. For TEP—LHCE, stronger salt-solvent interactions lead to more solvent decomposition, creating an organic-dominated SEI with poor passivation.

Diluents, typically fluorinated ethers or carbonates, are engineered to be electrochemically inert and nonsolvating. The efficacy of LHCEs hinges on the strategic selection of diluents that fulfill three critical criteria. [67] First, diluents must exhibit low donor numbers (<10 kcal mol⁻¹) to avoid coordinating with Li⁺ ions. This ensures they do not penetrate the primary solvation sheath or displace anions, thereby preserving the contact ion pairs and aggregates characteristic of HCEs. Second, diluents require moderate polarity (e.g., dielectric constants of 5–10) to ensure homogeneity with HCE solvents while minimizing free energy penalties for phase separation. Third, ideal diluents possess wide electrochemical windows (>4.5 V vs

16146840, 2025, 34, Downloaded from https://advanced.onlinelibrary

com/doi/10.1002/aenm.202502654 by HONG KONG POLYTECHNIC UNIVERSITY HU NG HOM, Wiley Online Library on [25/09/2025]. See the

onditions) on Wiley Online Library for rules of use; OA articles are governed by the applicable Creative Commons

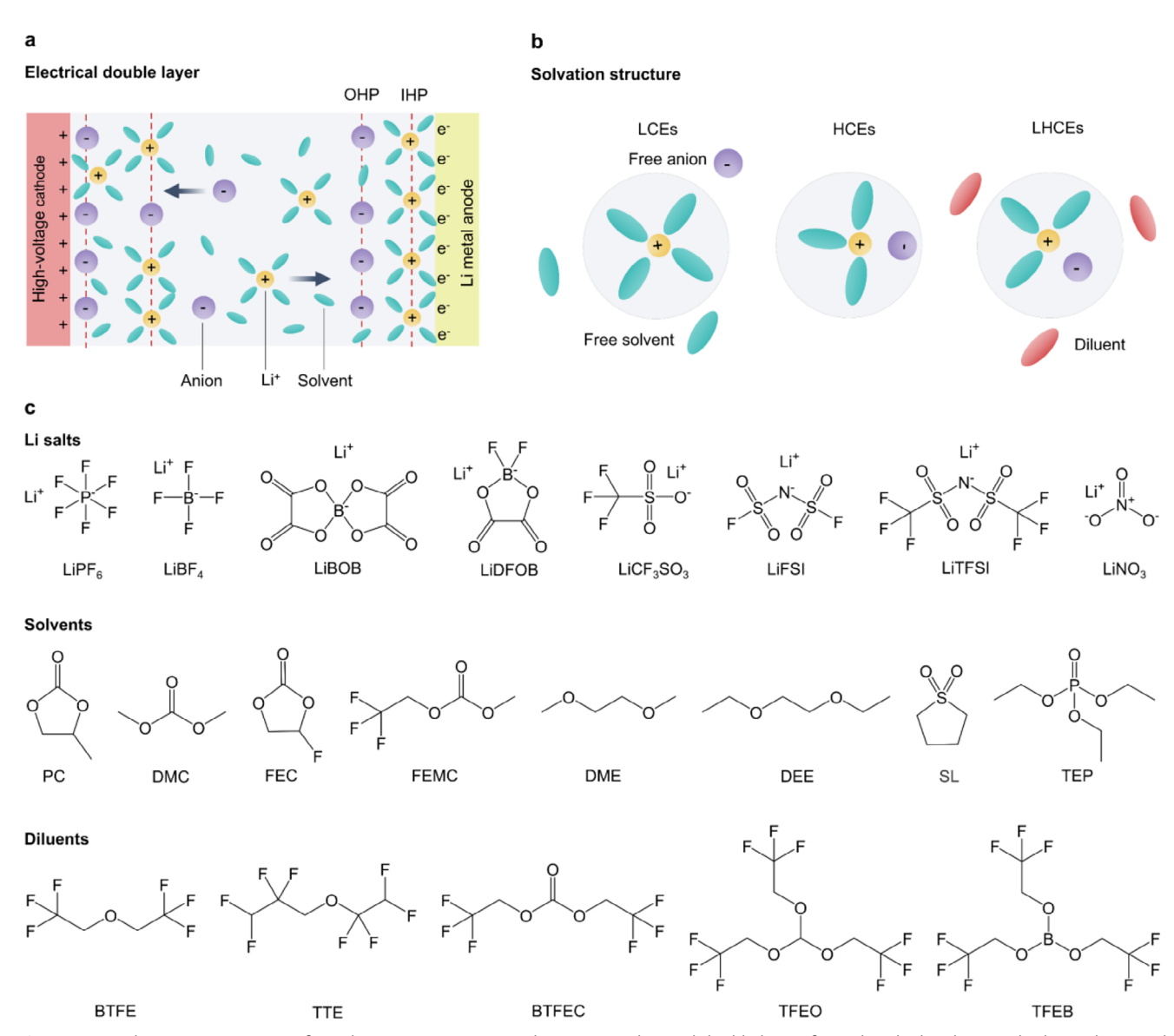


Figure 3. Regulating concentration of Li salts to prepare HCEs and LHCEs. a) Electrical double layers formed on high-voltage cathodes and Li metal anodes during charge process. The compounds in the inner Helmholtz plane (IHP) and outer Helmholtz plane (OHP) are closely related to the later formed interphase, which can be used to help develop better electrolytes to tune CEI or SEI properties. b) Solvation structures of three electrolytes: LCEs, HCEs, and LHCEs. c) Chemical structures of representative Li salts: LiPF₆, LiBF₄, lithium bis(oxalato)borate (LiBOB), lithium difluoro(oxalato)borate (LiDFOB), LiFSI, LiTFSI, and LiNO₃; solvents: DMC, PC, FEC, FEMC, DME, and ethylene glycol diethyl ether (DEE), sulfolane (SL), and triethyl phosphate (TEP); diluents: bis(2,2,2-trifluoroethyl) ether (BTFE), 1,1,2,2-tetrafluoroethyl-2,2,3,3-tetrafluoropropyl ether (TTE), bis(2,2,2-trifluoroethyl) carbonate (BTFEC), TFEO, and tri(2,2,2-trifluoroethyl) borate (TFEB).

Li/Li⁺) to resist reduction at the anode and oxidation at high-voltage cathodes. Typical diluents include bis(2,2,2-trifluoroethyl) ether (BTFE),^[81] 1,1,2,2-tetrafluoroethyl-2,2,3,3-tetrafluoropropyl ether (TTE),^[76] bis(2,2,2-trifluoroethyl) carbonate (BTFEC),^[86] TFEO,^[87] and tri(2,2,2-trifluoroethyl) borate (TFEB).^[86] The CE values show variations depending on the diluent selected, which follow the order as: 99.5% (TTE—LHCE) = 99.5% (TFEO—LHCE) > 99.4% (BTFE—LHCE) > 96.8% (BTFEC—LHCE) > 95.4% (TFEB—LHCE).^[86] This is because the fluorinated ethers including BTFE, TTE, and TFEO enable anion-dominated solvation structure (typical LHCEs), fluorinated carbonate BTFEC coordi-

nates with Li⁺ in a second solvation shell (pseudo-LHCEs), while fluorinated borate TFEB accelerates Li metal degradation because of its electron-deficient character.

HCEs and LHCEs are promising electrolytes for achieving high-voltage stability and enhanced safety in LMBs. Conventional LiPF₆-based electrolytes, while suppressing Al corrosion, generate HF that accelerates TM dissolution from cathodes, leading to capacity fading. Replacing LiPF₆ with stable salts such as LiFSI reduces HF but fails to protect Al foil at high voltages. [88] This dilemma was resolved by formulating a superconcentrated electrolyte with a 1:1.1 molar ratio of LiFSI to DMC. [89] This HCE

16146840, 2025, 34, Downloaded from https://advanced.onlinelibrary

10.1002acam.20.20264 by HONG KONG POLYTECHINC UNIVERSITY HU NG HOM, Wiley Online Library on [25.09.2025], See the Terms and Conditions (https://onlinelibrary.wiley.com/terms-and-conditions) on Wiley Online Library for rules of use; OA articles are governed by the applicable Creative Commons

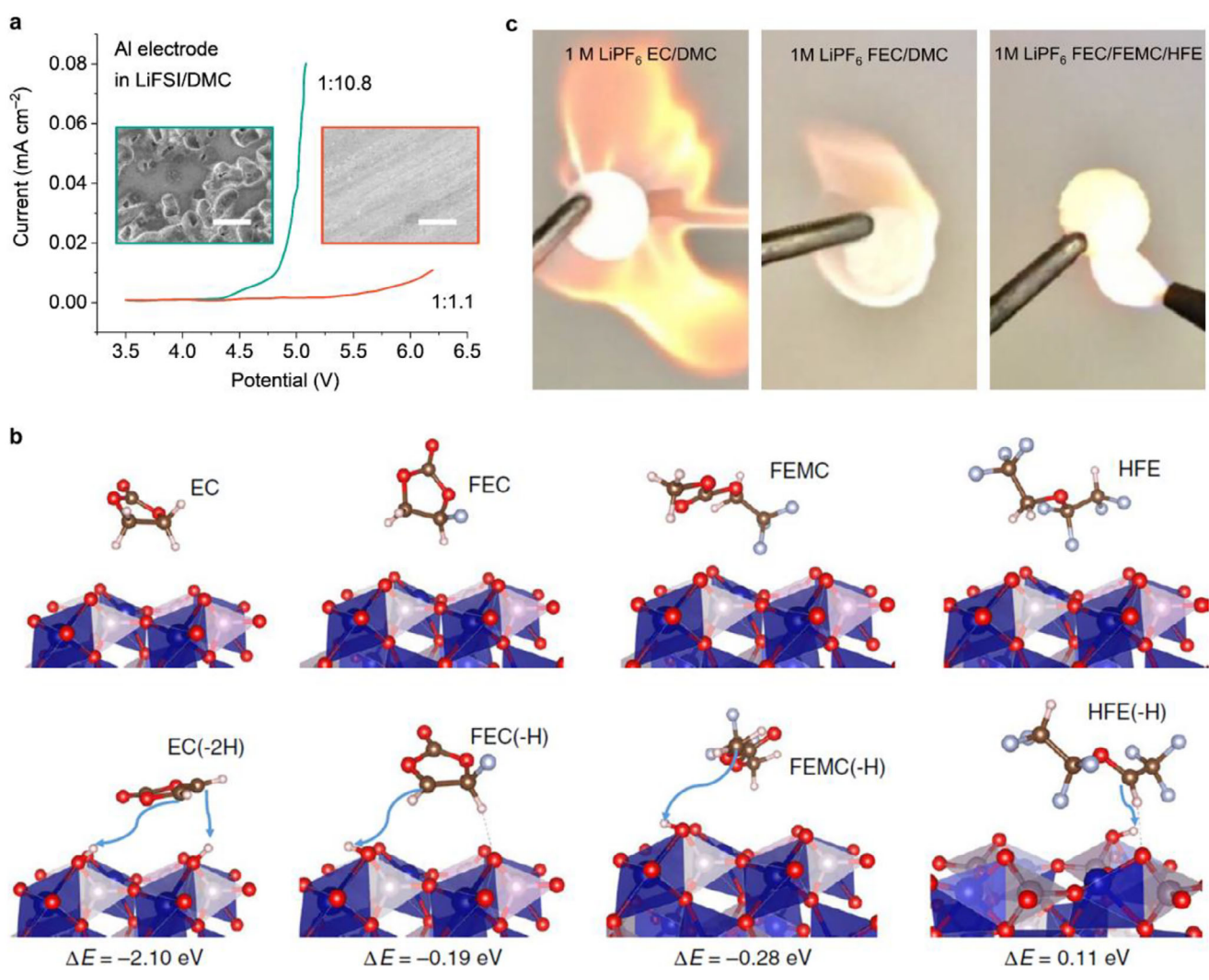


Figure 4. Performance of representative HCEs and LHCEs. a) Linear sweep voltammetry (LSV) of an Al electrode in various concentrations of LiFSI/DMC electrolytes in a three-electrode cell. The insets are scanning electron microscopy (SEM) images of the Al surface polarized in the dilute 1:10.8 and superconcentrated 1:1.1 electrolytes. Scale bars, 3 μm. Reproduced with permission.^[89] Copyright 2016, Nature Publishing Group. b) Reactivity of EC, FEC, FEMC, and HFE solvents at the fully charged CoPO₄ (010) surface from density functional theory (DFT) calculations. ΔE , the energy difference between the adsorbed solvent and reacted solvent. Reproduced with permission.^[29] Copyright 2018, Nature Publishing Group. c) Flammability tests for 1 μ LiPF₆ EC/DMC, 1 μ LiPF₆ FEC/DMC, and 1 μ LiPF₆ FEC/FEMC/HFE. Reproduced with permission.^[29] Copyright 2018, Nature Publishing Group.

electrolyte minimized free solvent and anions, inhibiting both Al corrosion and TM dissolution (Figure 4a). Consequently, the HCE demonstrated exceptional stability in LNMO/graphite full cells, achieving 95% capacity retention after 100 cycles at 4.6 V, and enhanced safety due to reduced flammability and volatility. Moreover, LHCEs such as 1 M LiFSI DME/TFEO electrolyte, could stabilize high-voltage NCM811 cathodes by forming a protective LiF-rich interphase, mitigating phase transitions and TM dissolution. [31] Meanwhile, the electrolyte's low viscosity and localized high-concentration characteristics ensured efficient ion transport and electrode wetting. The LHCEs enhanced safety, rate capability (up to 4 C, "1 C" refers to a charge or discharge rate where the battery's full capacity is delivered in 1 h), and cycling stability, advancing practical high-energy LMBs.

The development of a F-rich interphase is essential for optimizing electrolyte compatibility with Li metal anodes and high-

voltage cathodes. To achieve this, a nonflammable, all-fluorinated electrolyte was designed, comprising 1 м LiPF₆ in FEC, FEMC, and HFE at a 2:6:2 weight ratio.^[29] FEC, with its high polarity and dielectric constant, served as the primary solvating agent to dissociate LiPF6, while FEMC and HFE acted as diluents to enhance ionic conductivity and reduce viscosity. The fluorinated solvents contributed to the formation of a LiF-dominated SEI on the Li-metal anode, which suppresses dendrite growth by blocking electron tunneling and promoting uniform Li⁺ flux. Simultaneously, a fluorine-rich CEI formed on high-voltage cathodes, stabilizing the cathode surface against oxidative decomposition and TM dissolution. Quantum chemistry calculations revealed that fluorinated solvents exhibit higher oxidation stability and slower decomposition kinetics compared to conventional carbonate solvents, with higher energy barriers for hydrogen abstraction reactions on charged cathode surfaces, thereby stabilizing

16146840, 2025, 34, Downloaded from https

10.1002/aemm.202502654 by HONG KONG POLYTECHNIC UNIVERSITY HU NG HOM, Wiley Online Library on [25/09/2025]. See the Terms

nditions) on Wiley Online Library for rules of use; OA articles are governed by the applicable Creative Commons

F3EME

Figure 5. Designing structure of solvent molecules to prepare WSEs. a) Solvation structures of the strong solvating electrolytes (SSEs) and WSEs. Reduction potentials of free anions and aggregates. Reproduced with permission.^[91] Copyright 2023, Nature Publishing Group. b) Design scheme of weakly solvating fluorinated solvents: fluorinated FDMB and 1,5-dimethoxylpentane (FDMP), partial fluorinated-DEE family (F3DEE, F4DEE, F5DEE, and F6DEE), and fluorinated asymmetric ether (fluorinated 1-ethoxy-2-methoxyethane, F3EME).

asymmetric

structure

EME

aggressive cathodes (Figure 4b). Consequently, Li—LiCoPO₄ cells achieved 93% capacity retention after 1000 cycles at 5.0 V, far surpassing previous reports. Meanwhile, safety was enhanced by the electrolyte's nonflammability and superior thermal stability, confirmed via combustion tests (Figure 4c).

asymmetric

structure

For HCEs/LHCEs, anion-dominated solvation structures promote LiF-rich SEI/CEI formation, directly suppressing Li dendrite growth (Challenge 2.2) and electrolyte oxidation (Challenge 2.3). Meanwhile, reduced free solvents minimize flammability risks (Challenge 2.1), and reduced free anions prevent FSI-induced Al dissolution, resolving Al current collector corrosion (Challenge 2.3). Additionally, multisalt electrolytes leverage complementary properties of distinct Li salts to overcome limitations of single-salt systems, such as Al current collector corrosion, SEI/CEI instability, and narrow electrochemical windows.[88] For instance, LiFSI's high ionic conductivity and LiF-forming ability synergize with LiDFOB's capacity to form borate-rich CEI layers that suppress transition metal dissolution and Al corrosion at >4.5 V. Additionally, ternary-salt systems (e.g., LiPF₆/LiFSI/LiTFSI) leverage synergistic advantages to overcome individual salt limitations: LiPF₆ passivates Al, while

imide salts (LiFSI/LiTFSI) improve thermal stability and anion-derived interphases.

higher anodic and

cathodic stability

3.2. Designing Structure of Solvent Molecules to Prepare WSEs

Beyond HCEs and LHCEs, WSEs also promote the formation of an inorganic-dominated interphase, enhancing interfacial stability. WSEs are designed to reduce the interaction strength between solvent molecules and Li⁺ ions, thereby altering solvation structures to favor anion-dominated coordination and interfacial chemistry (**Figure 5a**). Unlike traditional electrolytes, where solvent molecules tightly bind to Li⁺ ions, WSEs promote the formation of aggregated ion clusters (Li⁺—anion cluster). This structural shift is achieved through molecular engineering strategies, such as fluorination, steric hindrance, and the use of solvents with low dielectric constants or donor numbers.^[90]

Conventional carbonate solvents exhibit HOMO energies above -7.5 eV (**Table 1**), rendering them susceptible to oxidation above 4.3 V. For instance, EC (HOMO = -7.21 eV) undergoes dehydrogenation at charged NMC811 surfaces, while fluorinated

MPE

16146840, 2025, 34, Downloaded from https://advanced.onlinelibrary.wiley.com/doi/10.1002/aemn.202902654 by HONG KONG POL YTECHNIC UNIVERSITY HU NG HOM, Wiley Online Library on [25/09/2025]. See the Terms

conv/terms-and-conditions) on Wiley Online Library for rules of use; OA articles are governed by the applicable Creative Commons

Table 1. DFT-calculated electronic properties and Li⁺ coordination energies of typical electrolyte solvents.

Solvent class	Typical molecule	HOMO [eV]	LUMO [eV]	Electrochemical window [V]	Binding energy [kcal mol ⁻¹]	Dielectric constant	Donor number
Carbonate	EC	-7.21	0.18	7.39	-34.2	89.6	16.6
Carbonate	DMC	-7.05	0.32	7.37	-28.7	3.1	17.5
Ether	DME	-6.88	-0.15	6.73	-36.5	7.2	24.0
Fluorinated	FDMB	-8.12	-0.87	7.25	-29.8	7.5	10.2
Ionic liquid	[EMIm][FSI]	-7.95	-1.02	6.93	-45.3	15.0	12.0

ethers like FDMB (HOMO = -8.12 eV) resist oxidation up to 6 V. The weak Li⁺ binding energy of FDMB (-29.8 kcal mol⁻¹) compared to DME (-36.5 kcal mol⁻¹) arises from electron-withdrawing $-\text{CF}_2-$ groups, which lower solvent donicity.^[34] This enables anion-aggregated solvation clusters even at 1 \upmu concentration (WSEs), facilitating FSI⁻ decomposition into LiF-rich SEI.

WSEs could be achieved by molecular design on rational engineering of fluorinated ether solvents. For example, a fluorinated molecule with low solvation ability was prepared by extending the alkyl chain of DME to reduce electron density on oxygen atoms and positioning fluorinated moieties

(—CF₂—) away from oxygen to maintain Li⁺ coordination ability (Figure 5b). [34] This architecture enabled unique Li—F interactions, which promote anion-dominated solvation structures with a high FSI⁻/solvent ratio. These features minimized free solvent decomposition, fostering an ultrathin (\approx 6 nm), fluorinerich SEI that suppresses dendrite growth. Simultaneously, the electron-withdrawing —CF₂— groups elevated the oxidation stability (>6 V), enabling compatibility with high-voltage cathodes (**Figure 6a**,b). Consequently, practical implementations exhibited outstanding performance: Li—NMC full cells with 50 μ m Li retained 90% capacity after 420 cycles, while industrial anode-free pouch cells achieved \approx 325 Wh kg⁻¹ energy

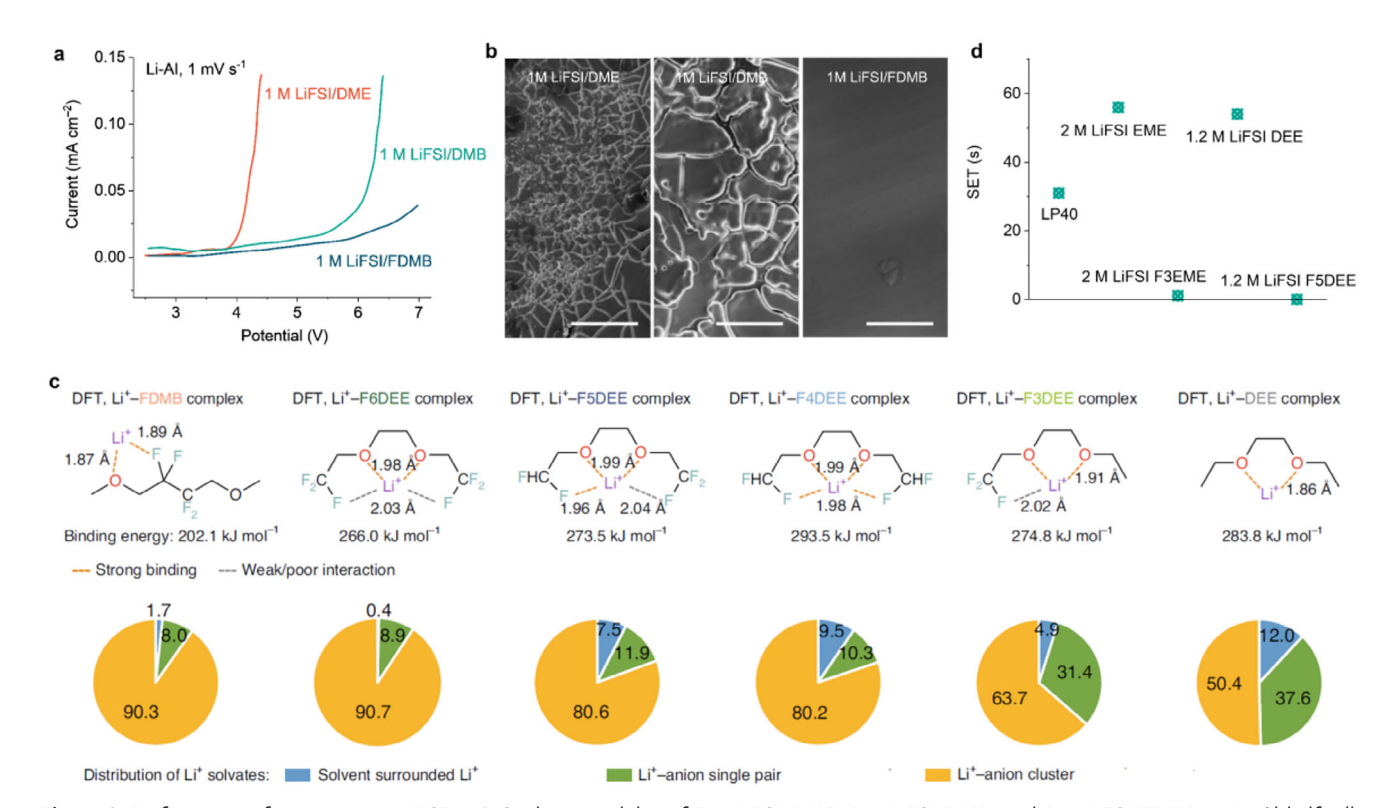


Figure 6. Performance of representative WSEs. a) Oxidation stability of 1 M LiFSI/DME, 1 M LiFSI/DMB, and 1 M LiFSI/FDMB in Li—Al half-cells detected by LSV. Reproduced with permission.^[34] Copyright 2020, Nature Publishing Group. b) Al corrosion test in the three electrolytes. Scale bars, 3 μm. Reproduced with permission.^[34] Copyright 2020, Nature Publishing Group. c) Coordination structures and binding energies between one Li⁺ ion and one solvent molecule calculated using DFT. Most probable solvation structures of the first Li⁺ solvation sheath from molecular dynamics (MD) simulations and the distribution of different Li⁺ solvates in 1 M LiFSI/FDMB, 1.2 M LiFSI/F6DEE, 1.2 M LiFSI/F5DEE, 1.2 M LiFSI/F4DEE, 1.2 M LiFSI/F3DEE, and 1.2 M LiFSI/DEE. Reproduced with permission.^[82] Copyright 2022, Nature Publishing Group. d) Self-extinguishing time (SET) test for commercial carbonate electrolyte (LP40), 2 M LiFSI in EME, 2 M LiFSI in F3EME, 1.2 M LiFSI in DEE, and 1.2 M LiFSI in F5DEE. Reproduced with permission.^[92] Copyright 2025, Nature Publishing Group.



www.advenergymat.de

density and 80% capacity retention after 100 cycles. The design combined low salt concentration (1 $\rm M$), nonflammability, and scalable synthesis, overcoming limitations of conventional HCEs.

Although fluorination enhances the compatibility of WSEs with both electrodes, it often results in reduced ionic conductivity. Accordingly, the fluorination degree of solvent molecules should be controlled precisely. By systematically tuning the position and degree of fluorination on the DEE backbone, the researchers identified that partially fluorinated -CHF2 groups, rather than fully fluorinated -CF₃, optimized electrolyte performance.^[82] Through repeated synthesis, fluorinated-DEE variants (F3DEE, F4DEE, F5DEE, F6DEE) were created, with F4DEE and F5DEE containing -CHF2 groups, exhibiting superior performance. DFT calculations revealed that -CHF2's asymmetric structure enabled stronger Li+-solvent interactions (shorter Li-F bonds) than -CF3, promoting efficient ion dissociation while maintaining weak overall solvation to minimize parasitic reactions (Figure 6c). This design balanced solvent polarity to stabilize anion-derived SEI and suppress Al corrosion, achieving >99.9% CE and rapid activation. These electrolytes enabled stable cycling under practical conditions: ≈270 cycles in 50 µm Li||high-loading NMC811 full cells and >140 cycles in anode-free Cu||LiFePO4 pouch cells at fast rates.

The asymmetric structure exhibits weaker and less uniform Li⁺ solvation due to steric hindrance and directional dipole effects compared with its symmetric counterpart, accelerating Li+ desolvation and charge transfer kinetics. Accordingly, asymmetric ether molecules, such as 1-ethoxy-2-methoxyethane (EME) and 1methoxy-2-propoxyethane were synthesized, structurally distinct from conventional symmetric ethers (e.g., DME, DEE).[92] Further optimization involved fluorinating the β -carbon of EME to create fluorinated 1-ethoxy-2-methoxyethane (F3EME), balancing solvation ability and oxidative stability. The asymmetry-induced dipole reorientation minimized solvent shielding at the Li surface, promoting faster Li+ redox kinetics. Combined with fluorination's electron-withdrawing effects, this design suppressed solvent decomposition and enabled stable cycling in high-voltage NMC811 cells and anode-free Cu||Ni95 pouch cells (600 cycles under electric vertical take-off and landing protocols). The electrolyte also exhibited desirable noninflammability with the SET value of almost zero (Figure 6d).

3.3. Applying Highly Stable ILs as Electrolyte Solvents

Conventional organic carbonate-based electrolytes face intrinsic limitations, including narrow electrochemical stability windows (<4.5 V), high flammability, and poor compatibility with Li metal anodes and high-voltage cathodes, which lead to severe safety risks and rapid capacity fading. ILs, composed of organic cations and inorganic/organic anions, have emerged as a transformative class of electrolyte solvents to address these issues, offering unique advantages such as nonflammability, negligible volatility, and wide electrochemical stability windows (up to 6 V). [93] Their tunable physicochemical properties, driven by anion—cation interactions, enable the design of advanced electrolytes that stabilize both Li metal anodes and high-voltage cathodes by forming robust, inorganic-rich

interphases. For Li metal anodes, FSI-- or TFSI--based ILs facilitate the decomposition of anions into LiF-, Li₃N-, and Li₂Odominated SEI layers (Figure 7a), which exhibit high mechanical strength and ionic conductivity to suppress dendrite propagation. Cations mainly include 1-ethyl-3-methylimidazolium [EMIm]⁺, [94,95] 1-methyl-1-propylpyrrolidinium [Pyr13]⁺, [96] 1,1diethylpyrrolidinium [Pyr22]⁺, [97] 1,1-dipropylpyrrolidinium [Pyr33]⁺,^{[97}] 1-butyl-1-methylpyrrolidin-1-ium $[Pyr14]^+, [98]$ [EMMP]+,[99] 3,3-difluoro-1-methyl-1-propylpyrrolidin-1-ium [DFPyr13]+,[100] and 4,4-difluoro-N-methyl-N-propylpiperidium [DFP13]⁺.[101] Asymmetric or heteroatom-containing cations (e.g., [EMIm]+, [Pyr14]+) undergo reductive decomposition at low potentials (<1.5 V vs Li/Li⁺), contributing organic species (e.g., alkyl lithium, Li₃N) to the SEI. Symmetric cations (e.g., [Pyr22]+, [Pyr33]+) resist reduction due to steric shielding and high LUMO energy levels. Instead, they adsorb onto Li protrusions, creating electrostatic shields that homogenize Li+ flux. At high-voltage cathodes, ILs resist oxidative decomposition, and form stable CEI rich in LiF and fluorinated organic species. which prevent electrolyte oxidation, TM dissolution, and oxygen release.

Despite these advantages of IL-based electrolytes, challenges persist, including high viscosity and interfacial incompatibility with Li metal anodes and high-voltage cathodes. To address these issues, the high-concentration and localized high-concentration strategies are applied. For example, an innovative IL electrolyte was reported, composed of EMIm cations, high-concentration FSI anions, and sodium bis(trifluoromethylsulfonyl)imide (NaTFSI) additive, termed "EM-5Li-Na." [94] This high-concentration design formed robust, fluorine-rich SEI/CEI layers containing LiF, Li₂S, Li₂CO₃, and trace NaF, which suppress parasitic reactions and enhance interfacial stability. Meanwhile, the Na+ ions in NaTFSI additive provided electrostatic shielding to mitigate Li dendrite growth. Additionally, the EM-5Li-Na displayed exceptional thermal stability and nonflammability, as confirmed by thermogravimetric analysis and combustion tests (Figure 8a,b). When paired with LCO cathodes, the electrolyte supported high discharge voltages (up to 4.4 V), retaining 81% capacity after 1200 cycles at 0.7 C even under high mass loadings (≈16 mg cm⁻²). Recent advances in localized concentrated IL electrolytes, which dilute ILs with low-viscosity cosolvents, improved ionic conductivity while retaining the SEI/CEI-forming advantages of IL-dominated solvation structures.[96,102]

Molecular design of ILs is another effective method to enhance the kinetics and interfacial compatibility. In this context, a novel approach involved the rational design of symmetric organic solvents, such as Pyr22FSI, which leverage strong cation–anion associations to minimize anion-dominated Li⁺ clusters (Figure 8c,d).^[97] This "miniature solvation" concept reduced desolvation energy barriers and enhanced ionic conductivity (6.31 mS cm⁻¹), outperforming traditional ILs. Meanwhile, the symmetric cation structure promoted compact electric double layers, enabling uniform anion distribution at the Li surface and fostering SEI layers rich in inorganic components (Li₃N, Li₂O, LiF), which suppress dendrites and mitigate side reactions. Electrolytes incorporating Pyr22FSI demonstrated exceptional cycling stability in practical cells, achieving 400 cycles with 88% capacity retention in

16146840, 2025, 34, Downloaded from https://advanced.onlinelibrary.wiley.com/doi/10.1002/aemn.202902654 by HONG KONG POL YTECHNIC UNIVERSITY HU NG HOM, Wiley Online Library on [25/09/2025]. See the Terms

conditions) on Wiley Online Library for rules of use; OA articles are governed by the applicable Creative Commons License

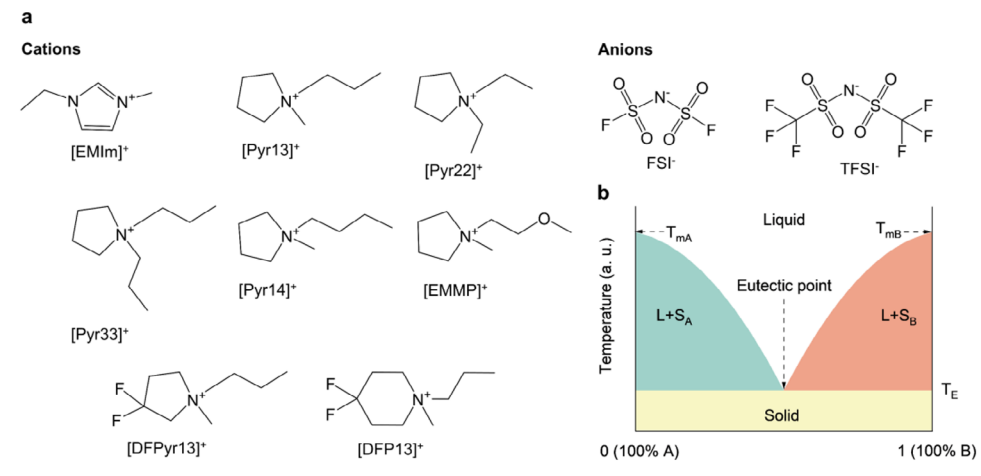


Figure 7. Applying highly stable ILs as electrolyte solvents. a) Cations and anions commonly used for the formulation of IL-based electrolytes. Cations: 1-ethyl-3-methylimidazolium [EMIm] $^+$, 1-methyl-1-propylpyrrolidinium [Pyr33] $^+$, 1,1-diethylpyrrolidinium [Pyr22] $^+$, 1,1-dipropylpyrrolidinium [Pyr33] $^+$, 1-butyl-1-methylpyrrolidin-1-ium [Pyr14] $^+$, 3,3-difluoro-1-methyl-1-propylpyrrolidin-1-ium [DFPyr13] $^+$, 4,4-difluoro-N-methyl-N-propylpiperidium [DFP13] $^+$. Anions: FSI $^-$ and TFSI $^-$. b) Proposed phase diagram of a eutectic mixture of two ILs, A and B. $T_{\rm m}$, melting point. S, solid phase. L, liquid phase. Binary mixtures of ILs could reduce the viscosity and melting point by generating the eutectic mixture ILs.

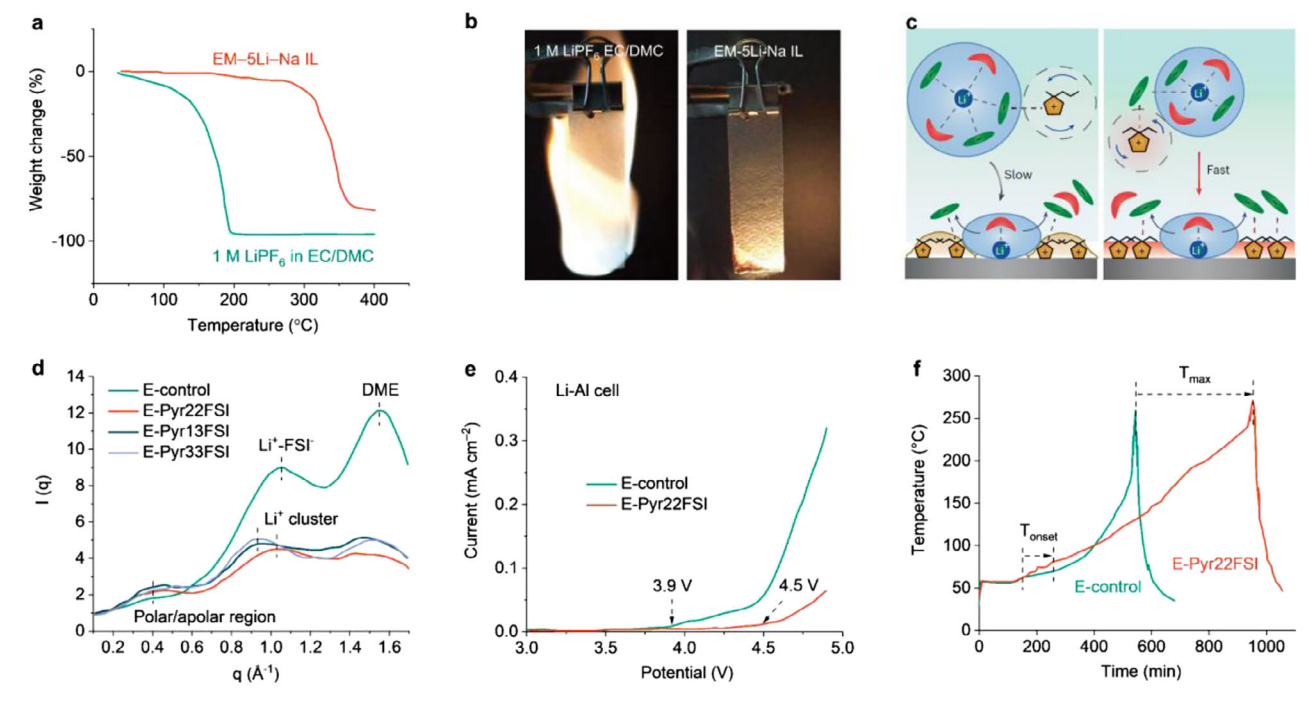


Figure 8. Performance of representative IL-based electrolytes. a) Thermal stability of EM—5Li—Na IL and conventional 1 μ LiPF₆ in EC/DMC electrolytes. Reproduced with permission.^[94] Copyright 2020, Wiley-VCH. b) Flammability tests of the EM—5Li—Na IL electrolytes and conventional electrolytes. Reproduced with permission.^[97] Copyright 2020, Wiley-VCH. c) Proposed Li⁺ solvation structures in E-Pyr13FSI and E-Pyr22FSI electrolytes. Reproduced with permission.^[97] Copyright 2025, Nature Publishing Group. d) Small-angle X-ray scattering spectra of the E-control, E-Pyr22FSI, E-Pyr13FSI, and E-Pyr33FSI electrolytes, where *q* represents the momentum transfer vector, and *I* represents the scattering intensity at that angle. Reproduced with permission.^[97] Copyright 2025, Nature Publishing Group. e) LSV scans for different electrolytes. The arrows indicate the oxidation onset potential of E-control (3.9 V) and E-Pyr22FSI (4.5 V), respectively. Reproduced with permission.^[97] Copyright 2025, Nature Publishing Group. f) Accelerating rate calorimeter (ARC) results of the charged Li-NCM811 pouch cell under thermal abuse conditions, where T_{onset} is the onset temperature of self-heating and T_{max} is the temperature at which the rising rate falls below 0.001 °C min⁻¹. Reproduced with permission.^[97] Copyright 2025, Nature Publishing Group.

16146840, 2025, 34, Downloaded from https://advanced.onlinelibrary.wiley.c

com/doi/10.1002/aenm.202502654 by HONG KONG POLYTECHNIC UNIVERSITY HU NG HOM, Wiley Online Library on [25.09/2025]. See the Terms and Conditions (https://onlinelibrary.wiley.com/doi/10.1002/aenm.202502654 by HONG KONG POLYTECHNIC UNIVERSITY HU NG HOM, Wiley Online Library on [25.09/2025]. See the Terms and Conditions (https://onlinelibrary.wiley.com/doi/10.1002/aenm.202502654 by HONG KONG POLYTECHNIC UNIVERSITY HU NG HOM, Wiley Online Library on [25.09/2025]. See the Terms and Conditions (https://onlinelibrary.wiley.com/doi/10.1002/aenm.202502654 by HONG KONG POLYTECHNIC UNIVERSITY HU NG HOM, Wiley Online Library on [25.09/2025]. See the Terms and Conditions (https://onlinelibrary.wiley.com/doi/10.1002/aenm.202502654 by HONG KONG POLYTECHNIC UNIVERSITY HU NG HOM, Wiley Online Library on [25.09/2025]. See the Terms and Conditions (https://onlinelibrary.wiley.com/doi/10.1002/aenm.202502654 by HONG KONG POLYTECHNIC UNIVERSITY HU NG HOM, Wiley Online Library on [25.09/2025]. See the Terms and Conditions (https://onlinelibrary.wiley.com/doi/10.1002/aenm.2025026).

com/terms-and-conditions) on Wiley Online Library for rules of use; OA articles are governed by the applicable Creative Commons

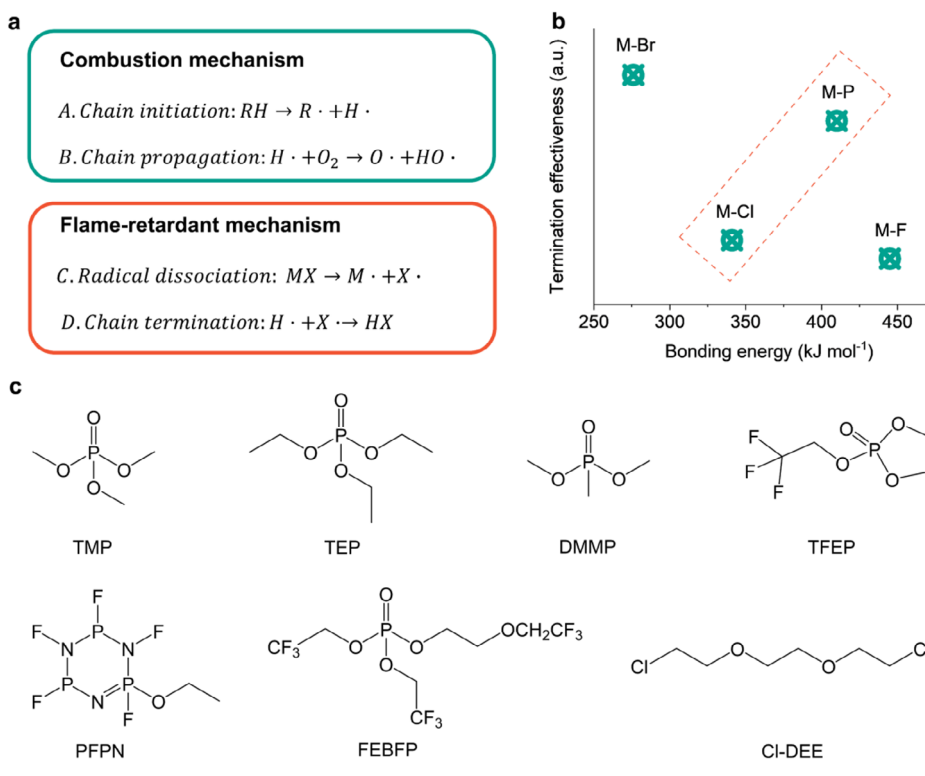


Figure 9. Applying flame-retardant P- or Cl-based molecules as electrolyte solvents. a) Combustion and flame retardant mechanisms. b) Termination effectiveness of various classes of scavengers: F-based solvents (M—F), Cl-based solvents (M—Cl), Br-based solvents (M—Br), and P-based solvents (M—P). Reproduced with permission. [103] Copyright 2024, Royal Society of Chemistry. c) Molecular formula commonly used for the formulation of flame-retardant electrolytes for LMBs: trimethyl phosphate (TMP), TEP, dimethyl methyl phosphonate (DMMP), 2-(2,2,2-trifluoroethoxy)-1,3,2dioxaphospholane 2-oxide (TFEP), ethoxy(pentafluoro) cyclotriphosphazene (PFPN), 2-(2,2,2-trifluoroethoxy)ethyl bis(2,2,2-trifluoroethyl) phosphate (FEBFP), and 1,2-bis(2-chloroethoxy)ethane (CI-DEE).

high-voltage NCM811 configurations under lean electrolyte conditions (E/C ratio \approx 2 g Ah⁻¹) and high power density (639.5 W kg⁻¹), which address the trade-off between energy density and rate capability (Figure 8e). Crucially, the nonflammable nature of Pyr22FSI-based electrolytes ensured safety, as demonstrated by nail penetration and accelerating rate calorimeter (ARC) tests where pouch cells exhibited no thermal runaway (Figure 8f).

Overall, the approaches including HCEs/LHCEs, WSEs, and ILs collectively manipulate Li⁺ coordination chemistry to achieve three shared objectives: 1) promoting inorganic-rich interphase formation; 2) suppressing free solvent reactivity; and 3) enhancing electrochemical stability. For instance, HCEs/LHCEs achieve this through massive salt excess (4-7 M) to force anion coordination; WSEs accomplish it via molecular engineering to intrinsically weaken solvent-Li+ binding; while ILs leverage cation-anion associations to create a prestructured, low-solvation environment.

3.4. Applying Flame-Retardant P- or Cl-Based Molecules as **Electrolyte Solvents**

Beyond strategies including HCEs, LHCEs, WSEs, and IL-based electrolytes to reduce flammability, flame-retardant electrolyte engineering offers another viable solution for improving the safety of LMBs. The design of flame-retardant electrolyte depends on two key points, including the flame retardant efficiency, and compatibility toward Li metal anodes and high-voltage cathodes. Combustion in battery systems originates from exothermic chain reactions propagated by highly reactive hydrogen radicals (H•), which are generated during thermal decomposition of organic electrolytes (RH \rightarrow R \bullet + H \bullet) (Figure 9a).^[103] These radicals react with oxygen to sustain a self-accelerating cycle, $H \bullet + O_2 \rightarrow O \bullet$ + HO•, thereby retaining the combustion process. Flame retardants function by disrupting these chain reactions through two continuous mechanisms: 1) radical scavenger dissociation (MX \rightarrow M• + X•), where the retardant releases quenching agents (X•) to neutralize H \bullet radicals, and 2) chain termination (H \bullet + X \bullet \rightarrow HX), where scavengers react with radicals to form stable, nonreactive species (HX).

F-based solvents, exhibit limited efficiency due to high dissociation energies of their scavenger bonds (C-F: 485 kJ mol⁻¹) and slower termination kinetics, resulting in delayed radical quenching and incomplete fire suppression (Figure 9b).[103] Br-based solvents show much higher termination effectiveness, because the C-Br bond's lower dissociation energy (276 kJ mol⁻¹) enables rapid release of Bro radicals during thermal stress, ensuring immediate availability for chain termination. However, the highly reactive Br-based solvents are not compatible with Li metal anodes, which leads to low CE of LMBs. By contrast, because of the highly flame-retardant efficiency and much better

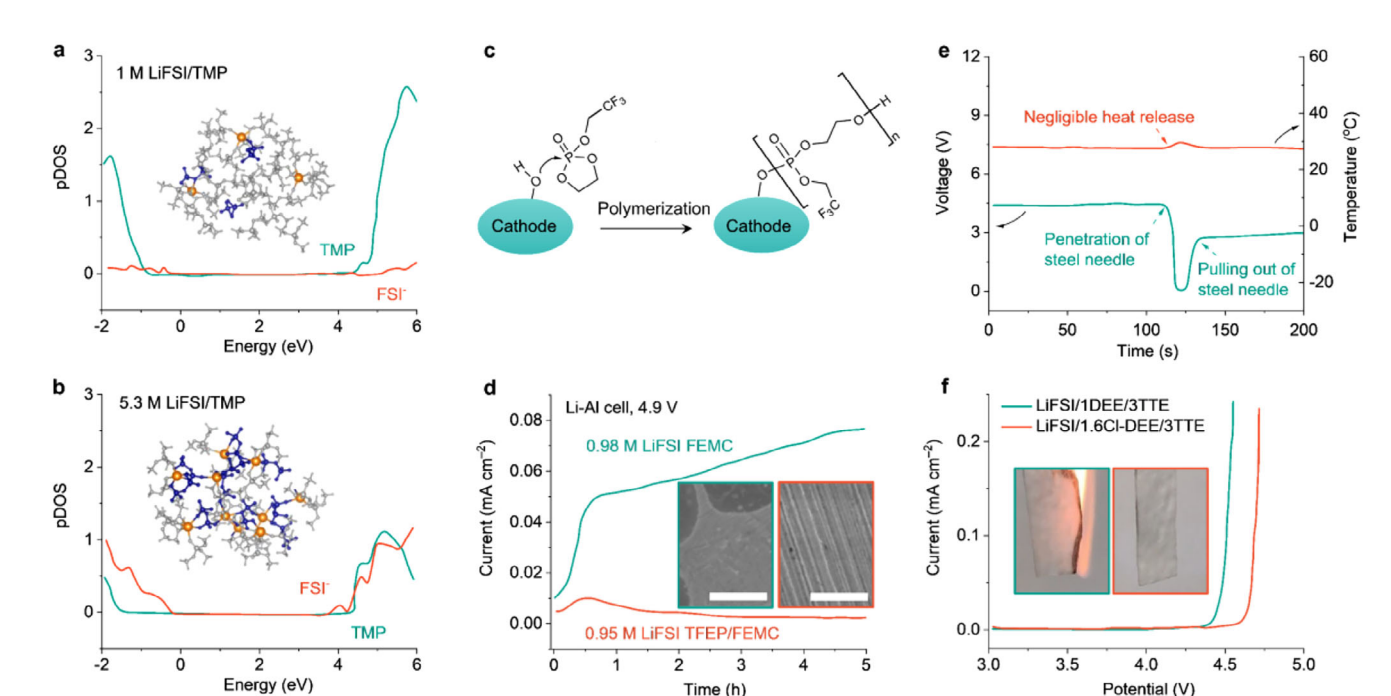


Figure 10. Performance of flame-retardant electrolytes. a,b) Projected density of states (pDOS) of (a) 1.0 m and (b) 5.3 m LiFSI/TMP electrolytes from DFT simulations. Reproduced with permission. [110] Copyright 2018, Nature Publishing Group. c) Schematic illustrations of the ring-opening polymerization of TFEP for formation of CEI layers. Reproduced with permission. [107] Copyright 2020, Nature Publishing Group. d) Chronoamperometry profiles of the Al—Li cells at 4.9 V in 0.98 m LiFSI FEMC and 0.95 m LiFSI TFEP/FEMC electrolytes after performing a LSV scan from the open circuit voltage to 4.9 V. Insets: SEM images of the Al foil after the chronoamperometry test. Scale bars, 3 μm. Reproduced with permission. [107] Copyright 2020, Nature Publishing Group. e) Nail penetration tests of fully charged Li—NCM811 pouch cells with 0.8 m lithium (fluorosulfonyl) (nonafluorobutanesulfonyl) imide (LiFN-FSI)/FEBFP electrolytes. Reproduced with permission. [109] Copyright 2024, Nature Publishing Group. f) Oxidation stability tests of LiFSI in 1DEE/3TTE and LiFSI in 1.6Cl—DEE/3TTE electrolytes on Super-P electrode using LSV. Insets: flammability tests of different ether-based electrolytes. Reproduced with permission. [111] Copyright 2022, Wiley-VCH.

compatibility toward Li metal anodes, P-based compounds are the main solvents to prepare flame-retardant electrolytes, including trimethyl phosphate (TMP), [104] TEP, [71,105] dimethyl methyl phosphonate (DMMP), [106] 2-(2,2,2-trifluoroethoxy)-1,3,2-dioxaphospholane 2-oxide (TFEP), [107] ethoxy(pentafluoro) cyclotriphosphazene (PFPN), [108] and 2-(2,2,2-trifluoroethoxy)ethyl bis(2,2,2-trifluoroethyl) phosphate (FEBFP) [109] (Figure 9c).

High-concentration and localized high-concentration strategies are critical for P-based electrolytes, as they could improve compatibility with Li metal anodes by tuning solvation structures. At high salt concentrations (e.g., 5.3 M LiFSI/TMP), the HCEs exhibited unique solvation structures, where >95% of TMP molecules coordinate with Li+, forming a 3D network that suppresses free solvent availability (Figure 10a,b).[110] This structure enabled the spontaneous formation of a robust, inorganic SEI on anodes through preferential reduction of FSI- rather than the TMP solvent. The inorganic SEI replaces the conventional organic-inorganic hybrid SEI derived from carbonate solvents, which are thermally unstable and prone to decomposition. Importantly, the concentrated electrolytes eliminated flammable components, rendering them intrinsically nonflammable with no measurable flash point (>200 °C) and zero STE. They acted as fire extinguishers at high temperatures, as TMP vapor suppresses combustion by scavenging reactive radicals. Meanwhile, Li-based cells showed negligible capacity loss over 1000 cycles (13 months) and 99.6% efficiency. Additionally, LHCEs could retain the advantages of HCEs, such as nonflammability and wide electrochemical stability, while overcoming their limitations of high viscosity, poor wettability, and cost. The LHCE's unique solvation structure (e.g., 1 m LiFSI in TEP/BTFE), localized Li⁺—TEP—FSI coordination preserved by the inert diluent BTFE, facilitated a robust, LiF-rich SEI that suppresses dendrite formation and parasitic reactions.^[105] As a result, the LHCE resisted oxidation up to 5.0 V, mitigating Al corrosion and enabling compatibility with high-voltage cathodes such as NMC622, with >97% capacity after 600 cycles at 1 C. The electrolyte's fire-retardant properties, confirmed by flame tests, addressed critical safety concerns.

Molecular design of flame-retardant solvents represents another effective strategy for enhancing the cycling stability of high-voltage LMBs. A novel TFEP solvent was synthesized by combining structural features of cyclic carbonates (for SEI formation) with phosphate-based flame-retardant properties and fluorination to enhance oxidative stability. The electrolyte formulation, 0.95 M LiFSI in a TFEP/FEMC mixture (1:3 by volume), demonstrated exceptional nonflammability (zero SET) and high thermal stability. Meanwhile, TFEP's cyclic structure enabled reduction at ≈ 1 V during initial lithiation, forming a LiFand LiPO $_x$ -rich SEI. TFEP's chemical polymerization on cathode surfaces formed a protective CEI, mitigating TM dissolution and electrolyte oxidation (Figure 10c). The electrolyte suppressed Al corrosion up to 5.4 V by forming a passivation layer





www.advenergymat.de

(AlF3 and LiF) via TFEP decomposition, overcoming a major limitation of imide salts such as LiFSI, which typically corrode Al at >4 V (Figure 10d). Consequently, the electrolyte enabled stable cycling of NMC111 at 4.5 V (80.1% capacity retention after 500 cycles) and LNMO at 4.9 V (70% retention after 200 cycles). Moreover, a novel FEBFP was designed a by covalently bonding three critical functional moieties: 1) a flameretardant phosphate group (-(RO)₃-P=O), 2) a flexible ether chain (-CH2-CH2-O-CH2CF3) to enhance Li+ transport and electrode compatibility, and 3) fluorinated alkyl groups (-CF₃) to improve thermal stability and oxidative resistance.[109] The lithium (fluorosulfonyl)(nonafluorobutanesulfonyl)imide (LiFN-FSI) salt was thereafter chosen for its unique anion structure, which combines fluorosulfonyl (-FSO₂) and perfluorinated alkylsulfonyl (-n-C₄F₉SO₂) groups. This fluorinated imide salt exhibited a higher reduction potential than the FEBFP solvent, enabling preferential decomposition at both electrodes to form LiF-rich SEI and CEI. LiF was mechanically robust, chemically inert, and thermally stable, which suppresses Li dendrite growth and mitigates parasitic reactions at high voltages. Additionally, the large, asymmetric structure of the FNFSI- anion weakened Li+-anion interactions, promoting salt dissociation and enhancing ionic conductivity (3.9 mS cm⁻¹) despite the relatively low salt concentration (0.8 M). The absence of volatile or flammable components allowed Li-LiFePO4 cells to function at 90 °C with minimal capacity fade, while 5.0 V LNMO cells achieve 200 cycles without decay. Safety tests, including nail penetration and ARC, confirmed no thermal runaway or gas evolution, revealing the success of the design (Figure 10e).

Cl-based compounds are emerging solvents for preparing high-voltage and flame-retardant electrolytes. Traditional ethers such as DME exhibit poor oxidative stability due to the high electron density on oxygen atoms, which elevates their HOMO energy levels and facilitates oxidation at high voltages. Fluorination, a common strategy to lower HOMO levels, compromises Li+ coordination and salt solubility due to fluorine's extreme electronegativity (3.98) and weak electron-donating ability. By contrast, Cl's moderate electronegativity (3.16) enables a balanced approach: Cl withdraws electron density from oxygen atoms (lowering HOMO levels and improving oxidation stability) while preserving Li⁺ coordination strength. Additionally, the lower C-Cl bond energy (83.7 kcal mol⁻¹ vs C-F: 115 kcal mol⁻¹) implies the higher tendency to cleave under combustion to release Cl. radicals, which scavenge reactive H. and HO• radicals, interrupting chain reactions and endowing flameretardant properties. For example, 1,2-bis(2-chloroethoxy)ethane (Cl-DEE) was rationally designed, a chlorinated derivative of the base molecule DEE, to enhance oxidation stability, flame retardancy, and interfacial compatibility while maintaining favorable Li+ solvation capability.[111] This design elevated the flashpoint of Cl-DEE to 126 °C (vs DEE: 35 °C), achieving intrinsic nonflammability (Figure 10f). The electrolyte formulation LiFSI/1.6Cl-DEE/3TTE LHCE further optimized performance by pairing Cl-DEE with the TTE diluent to reduce free solvent molecules while maintaining a high LiFSI salt concentration. The electrolyte formed dual inorganic-rich interphases, including a CEI dominated by LiF and LiCl, and a LiF-rich SEI. These interphases synergistically inhibited TM dissolution and Li dendrite growth. Consequently, the electrolyte stabilized

NMC811 cathodes at 4.6 V, achieving 88% capacity retention over 200 cycles.

Overall, phosphorus-based solvents (e.g., TEP, FEBFP) decompose to release PO· radicals, which quench H·/HO· combustion propagators. This reduces heat release rate by >60% and enables SET of 0 s. Chlorinated solvents (e.g., Cl—DEE) cleave C—Cl bonds to generate Cl· radicals, terminating chain reactions and increasing ignition resistance. HCEs/LHCEs minimize free solvents, reducing fuel for combustion. Ionic liquids show inherent nonflammability and high thermal stability (>400 °C) eliminate vapor-phase reactions.

4. Conclusions and Perspectives

The development of advanced liquid electrolytes for high-voltage LMBs is promising for enabling next-generation energy storage systems that show high energy density, long cycle life, and intrinsic safety. Although Li metal anodes and high-voltage cathodes offer ultrahigh theoretical capacities and operating voltages, their practical implementation is hindered by interrelated challenges at the interphases. Moreover, the flammability and volatility of traditional organic solvents, coupled with dendritic Li propagation, create severe safety hazards under thermal or mechanical abuse. Addressing these challenges requires a comprehensive electrolyte design strategy that simultaneously stabilizes both electrodes, enhances interfacial compatibility, and eliminates fire risks. HCEs and LHCEs leverage concentrated Li salts to minimize free solvent molecules, thereby reducing solvent decomposition at Li metal anodes and enhancing oxidative stability at high-voltage cathodes (Table 2). The unique solvation structure promotes anion-dominated SEI/CEI formation, enriching interfaces with LiF and other inorganic components that improve mechanical robustness and Li+ transport. WSEs, designed with fluorinated or sterically hindered solvents, decouple Li+-solvent interactions to facilitate anion decomposition, enabling the formation of ultrathin, inorganic-rich interphases. ILs, with their negligible volatility, nonflammability, and wide electrochemical windows, offer another solution for high-voltage and high-safety operation. Flame-retardant solvents, such as P- or Cl-containing compounds, effectively suppress electrolyte combustion.

Despite these advances, critical gaps remain in translating labscale innovations to practical high-safety and high-voltage LMBs. First, the interplay between Li⁺ solvation structure, interfacial chemistry, and long-term cycling stability requires deeper mechanistic understanding. For example, while anion-derived SEI/CEI layers (e.g., LiF, Li₂O, Li₃N) are widely acknowledged for their stability, the dynamic evolution of these interfaces under high current densities or extreme temperatures remains poorly characterized. Second, the scalability of advanced electrolytes, particularly those involving costly fluorinated solvents, ILs, or multistep synthetic routes, poses a significant barrier to commercialization. Third, the compatibility of advanced electrolytes with emerging high-voltage cathode materials (e.g., Li-rich manganese oxides) remains underexplored. Fourth, while intrinsic safety could be improved through nonflammable solvents or flame-retardant solvents, the interplay between electrolyte chemistry and thermal runaway mechanisms, particularly under abusive conditions such as nail penetration or crush tests, demands systematic study. Fifth, the combination of computational modeling,

16146840, 2025, 34, Downloaded from https://advanced.onlinelibrary.wiley.com/doi/10.1002/acmm.202302564 by HONG KONG POL YTECHNIC UNIVERSITY HU NG HOM, Wiley Online Library on [25.09/2025]. See the Terms and Conditions (https://onlinelibrary.wiley.com/terms-and-conditions) on Wiley Online Library for rules of use, OA articles are governed by the applicable Centwice Commons Licensein

Table 2. Key physicochemical properties of proposed electrolytes in this review, comparing ionic conductivity (δ), viscosity (μ), electrochemical window (E), Li⁺ transference number (t_1), and wettability.

Electrolyte type	Representative formulation	δ [mS cm $^{-1}$]	μ [cP]	E [V]	t _{Li} +	Wettability	Performance implications
HCEs	4 м LiFSI/DME	1.5–3.0	80–120	4.0-5.0	0.3-0.5	Low	LiF-rich SEI/CEI, limited rate capability
LHCEs	1 м LiFSI/DME/TTE	3.0-6.0	10-30	4.5-5.5	0.4-0.6	High	Balanced ion transport and stability
WSEs	1 м LiFSI/FDMB	2.0–4.0	5–15	>6.0	0.4–0.6	High	Thin SEI, high-voltage stability, low volatility
ILs	1 м LiFSI/Pyr22FSI	2.0-4.3	50–100	>5.5	0.2–0.4	Low	Nonflammable, wide stability window, high viscosity
Flame-retardant	1 м LiFSI/TFEP/FEMC	2.5–4.0	20–40	4.5–5.4	0.3-0.5	Moderate	Nonflammable, mitigates Al corrosion

machine learning, and high-throughput experimentation holds significant potential to accelerate electrolyte discovery but is underexplored. Finally, sustainability is also significant in electrolyte design, as the environmental impact of fluorinated solvents, ionic liquids, and Li salts could offset the green benefits of LMBs.

Accordingly, guidelines for future electrolyte design are proposed, offering actionable strategies across seven key dimensions. First, predictive methodologies can rapidly identify high-performance formulations since traditional trial-and-error approaches are inefficient. Machine learning models trained on databases of solvent properties (donor number, LUMO/HOMO levels) and cycling performance can accelerate the discovery of novel solvents. High-throughput robotic platforms should screen anion/solvent combinations for synergistic effects (e.g., FSIwith fluorinated ethers). Second, future research must prioritize understanding the dynamic evolution of interphases under operational conditions. Advanced in situ/operando techniques (e.g., cryo-electron microscopy, synchrotron X-ray diffraction, neutron depth profiling) should be employed to map spatial/temporal changes in SEI/CEI composition during cycling, especially under high current densities (>5 mA cm⁻²) or extreme temperatures (-20-80 °C). Computational studies (DFT/molecular dynamics (MD)) must model degradation pathways of anions/solvents at reactive interfaces to predict interphase stability. This addresses gaps in understanding how inorganic-rich interphases (e.g., LiF, Li₃N) evolve during long-term cycling, which is critical for mitigating dead Li formation and cathode degradation. Third, safety protocols must simulate real-world abuse scenarios. Standardized full-cell safety assessments, including nail penetration, crush tests, and accelerating rate calorimetry, should quantify thermal runaway thresholds (e.g., T_{onset} , self-heating rates). Fourth, electrolyte design must align with practical cell configurations to accelerate commercialization. Formulations should be optimized under lean-electrolyte conditions (<3 g Ah⁻¹), ultrathin Li anodes (<50 µm), and high-loading cathodes (>4 mAh cm⁻²). Cost analysis for fluorinated solvents/ILs should guide scalable synthesis routes, such as one-pot fluorination or wastefree IL production. Fifth, environmental impact must be central to material selection. Prioritize bioderived solvents (e.g., γ valerolactone) and recyclable ILs. Life-cycle assessments should evaluate carbon footprints of fluorinated compounds. Closedloop recycling protocols for Li salts/solvents will align with circular economy principles. Sixth, future work should prioritize

cathode-specific electrolyte screening. The distinct degradation modes of spinel versus layered cathodes demand specialized electrolyte approaches. LNMO benefits from fluorinated phosphates and chlorinated ethers that form hybrid CEI suppressing Mn dissolution, while layered NMC/LCO achieves stability via borate additives and ILs that mitigate TM dissolution and oxygen loss. Machine learning could accelerate the discovery of tailored CEI-forming additives. Finally, gel electrolytes, incorporating polymer matrices (e.g., poly(vinylidene difluoride-co-hexafluoropropene), poly(ethylene oxide), polymethyl methacrylate) infused with liquid electrolytes, offer a compelling trade-off between the high ionic conductivity of liquids and the enhanced safety/mechanical stability of solids, which also show great promise for future electrolyte design.

In conclusion, by integrating multifunctional solvents, stable Li salts, and optimized concentration, next-generation electrolytes can unlock the full potential of Li metal anodes and high-voltage cathodes while eliminating safety compromises. Bridging the gap between fundamental insights and industrial scalability, through interdisciplinary collaboration and sustainable innovation, will ultimately pave the way for LMBs to power electric vehicles, renewable energy grids, portable electronics, and beyond, serving a new era of energy-dense, durable, and inherently safe battery technologies.

Acknowledgements

The authors acknowledge the financial support from the NSFC/RGC Collaborative Research Scheme (Grant No. CRS_PolyU504/22), the RGC Research Impact Fund (Grant No. R5019-22), The National Natural Science Foundation of China (Grant No. 52203318), and the Hong Kong Polytechnic University (Grant No. 1-W22M; Grant No. 1.12.56.BDYU).

Conflict of Interest

The authors declare no conflict of interest.

Data Availability Statement

The data that support the findings of this study are available from the corresponding author upon reasonable request.

Keywords

high safety, high voltage, interphase, liquid electrolyte, lithium metal battery

16146840, 2025, 34, Downloaded from https://advanced.onlinelibrary.wiley

com/doi/10.1002/aenm.202502654 by HONG KONG POL YTECHNIC UNIVERSITY HU NG HOM, Wiley Online Library on [25/09/2025]. See the Terms

) on Wiley Online Library for rules of use; OA articles are governed by the applicable Creative



Received: May 14, 2025 Revised: June 23, 2025 Published online: July 10, 2025

- [1] J. Liu, Z. Bao, Y. Cui, E. J. Dufek, J. B. Goodenough, P. Khalifah, Q. Li, B. Y. Liaw, P. Liu, A. Manthiram, Y. S. Meng, V. R. Subramanian, M. F. Toney, V. V. Viswanathan, M. S. Whittingham, J. Xiao, W. Xu, J. Yang, X.-Q. Yang, J.-G. Zhang, *Nat. Energy* 2019, 4, 180.
- [2] X.-B. Cheng, R. Zhang, C.-Z. Zhao, Q. Zhang, Chem. Rev. 2017, 117, 10403.
- [3] J. W. Choi, D. Aurbach, Nat. Rev. Mater. 2016, 1, 16013.
- [4] Y. Jie, C. Tang, Y. Xu, Y. Guo, W. Li, Y. Chen, H. Jia, J. Zhang, M. Yang, R. Cao, Y. Lu, J. Cho, S. Jiao, Angew. Chem., Int. Ed. 2023, 63, 202307802.
- [5] S. Yuan, T. Kong, Y. Zhang, P. Dong, Y. Zhang, X. Dong, Y. Wang, Y. Xia, Angew. Chem., Int. Ed. 2021, 60, 25624.
- [6] M. Winter, B. Barnett, K. Xu, Chem. Rev. 2018, 118, 11433.
- [7] S. J. Tan, W. P. Wang, Y. F. Tian, S. Xin, Y. G. Guo, Adv. Funct. Mater. 2021, 31, 2105253.
- [8] X. Fan, C. Wang, Chem. Soc. Rev. 2021, 50, 10486.
- [9] J.-G. Zhang, W. Xu, J. Xiao, X. Cao, J. Liu, Chem. Rev. 2020, 120, 13312
- [10] X. Feng, D. Ren, X. He, M. Ouyang, Joule 2020, 4, 743.
- [11] Q. Zhao, S. Stalin, C.-Z. Zhao, L. A. Archer, Nat. Rev. Mater. 2020, 5,
- [12] L.-Z. Fan, H. He, C.-W. Nan, Nat. Rev. Mater. 2021, 6, 1003.
- [13] Z. Wang, Z. Sun, J. Li, Y. Shi, C. Sun, B. An, H.-M. Cheng, F. Li, Chem. Soc. Rev. 2021, 50, 3178.
- [14] Z. Wei, D. Yuan, X. Yuan, Y. Zhang, J. Ma, S. Zhang, H. Zhang, Chem. Soc. Rev. 2025, 54, 3775.
- [15] H. Wang, Z. Yu, X. Kong, S. C. Kim, D. T. Boyle, J. Qin, Z. Bao, Y. Cui, Joule 2022, 6, 588.
- [16] Z. Zhang, Y. Li, R. Xu, W. Zhou, Y. Li, S. T. Oyakhire, Y. Wu, J. Xu, H. Wang, Z. Yu, D. T. Boyle, W. Huang, Y. Ye, H. Chen, J. Wan, Z. Bao, W. Chiu, Y. Cui, *Science* 2022, 375, 66.
- [17] P. Zhai, L. Liu, X. Gu, T. Wang, Y. Gong, Adv. Energy Mater. 2020, 10, 2001257
- [18] J. Xiao, Q. Li, Y. Bi, M. Cai, B. Dunn, T. Glossmann, J. Liu, T. Osaka, R. Sugiura, B. Wu, J. Yang, J.-G. Zhang, M. S. Whittingham, *Nat. Energy* 2020, 5, 561.
- [19] S. Yuan, K. Ding, X. Zeng, D. Bin, Y. Zhang, P. Dong, Y. Wang, Adv. Mater. 2023, 35, 2206228.
- [20] S. Zhang, S. Li, Y. Lu, eScience 2021, 1, 163.
- [21] R. Gond, W. van Ekeren, R. Mogensen, A. J. Naylor, R. Younesi, Mater. Horiz. 2021, 8, 2913.
- [22] J. Chen, A. Naveed, Y. Nuli, J. Yang, J. Wang, Energy Storage Mater. 2020, 31, 382.
- [23] Y. S. Meng, V. Srinivasan, K. Xu, Science 2022, 378, 1065.
- [24] G. M. Hobold, J. Lopez, R. Guo, N. Minafra, A. Banerjee, Y. Shirley Meng, Y. Shao-Horn, B. M. Gallant, Nat. Energy 2021, 6, 951.
- [25] Y. Wang, X. Yang, Y. Meng, Z. Wen, R. Han, X. Hu, B. Sun, F. Kang, B. Li, D. Zhou, C. Wang, G. Wang, Chem. Rev. 2024, 124, 3494.
- [26] H. Wan, J. Xu, C. Wang, Nat. Rev. Chem. 2023, 8, 30.
- [27] F. Ding, W. Xu, X. Chen, J. Zhang, M. H. Engelhard, Y. Zhang, B. R. Johnson, J. V. Crum, T. A. Blake, X. Liu, J.-G. Zhang, J. Electrochem. Soc. 2013, 160, A1894.
- [28] Z. Zhang, L. Hu, H. Wu, W. Weng, M. Koh, P. C. Redfern, L. A. Curtiss, K. Amine, *Energy Environ. Sci.* 2013, 6, 1806.
- [29] X. Fan, L. Chen, O. Borodin, X. Ji, J. Chen, S. Hou, T. Deng, J. Zheng, C. Yang, S.-C. Liou, K. Amine, K. Xu, C. Wang, *Nat. Nanotechnol.* 2018, 13, 715.

- [30] J. Qian, W. A. Henderson, W. Xu, P. Bhattacharya, M. Engelhard, O. Borodin, J.-G. Zhang, Nat. Commun. 2015, 6, 6362.
- [31] X. Cao, X. Ren, L. Zou, M. H. Engelhard, W. Huang, H. Wang, B. E. Matthews, H. Lee, C. Niu, B. W. Arey, Y. Cui, C. Wang, J. Xiao, J. Liu, W. Xu, J.-G. Zhang, *Nat. Energy* **2019**, *4*, 796.
- [32] S. Yang, Y. Zhang, Z. Li, N. Takenaka, Y. Liu, H. Zou, W. Chen, M. Du, X.-J. Hong, R. Shang, E. Nakamura, Y.-P. Cai, Y.-Q. Lan, Q. Zheng, Y. Yamada, A. Yamada, ACS Energy Lett. 2021, 6, 1811.
- [33] J. Wang, Q. Zheng, M. Fang, S. Ko, Y. Yamada, A. Yamada, Adv. Sci. 2021, 8, 2101646.
- [34] Z. Yu, H. Wang, X. Kong, W. Huang, Y. Tsao, D. G. Mackanic, K. Wang, X. Wang, W. Huang, S. Choudhury, Y. Zheng, C. V. Amanchukwu, S. T. Hung, Y. Ma, E. G. Lomeli, J. Qin, Y. Cui, Z. Bao, Nat. Energy 2020, 5, 526.
- [35] W. Li, H. Yao, K. Yan, G. Zheng, Z. Liang, Y.-M. Chiang, Y. Cui, Nat. Commun. 2015, 6, 7436.
- [36] K. Xu, Chem. Rev. 2014, 114, 11503.
- [37] J. Xiao, N. Adelstein, Y. Bi, W. Bian, J. Cabana, C. L. Cobb, Y. Cui, S. J. Dillon, M. M. Doeff, S. M. Islam, K. Leung, M. Li, F. Lin, J. Liu, H. Luo, A. C. Marschilok, Y. S. Meng, Y. Qi, R. Sahore, K. G. Sprenger, R. C. Tenent, M. F. Toney, W. Tong, L. F. Wan, C. Wang, S. E. Weitzner, B. Wu, Y. Xu, Nat. Energy 2024, 9, 1463.
- [38] Z. Song, X. Wang, W. Feng, M. Armand, Z. Zhou, H. Zhang, Adv. Mater. 2024, 36, 2310245.
- [39] J. B. Goodenough, Y. Kim, Chem. Mater. 2009, 22, 587.
- [40] S. Kim, J.-A. Lee, T. K. Lee, K. Baek, J. Kim, B. Kim, J. H. Byun, H.-W. Lee, S. J. Kang, J.-A. Choi, S.-Y. Lee, M.-H. Choi, J.-H. Lee, N.-S. Choi, Energy Environ. Sci. 2023, 16, 5108.
- [41] X. Feng, M. Ouyang, X. Liu, L. Lu, Y. Xia, X. He, Energy Storage Mater. 2018, 10, 246.
- [42] D. Lin, Y. Liu, Y. Cui, Nat. Nanotechnol. 2017, 12, 194.
- [43] J. Zheng, M. S. Kim, Z. Tu, S. Choudhury, T. Tang, L. A. Archer, *Chem. Soc. Rev.* 2020, 49, 2701.
- [44] L. Hu, J. Deng, Q. Liang, J. Wu, B. Ge, Q. Liu, G. Chen, X. Yu, *EcoMat* 2022, 5, 12269.
- [45] X. Hu, Y. Gao, B. Zhang, L. Shi, Q. Li, EcoMat 2022, 4, 12264.
- [46] X. Gao, Y.-N. Zhou, D. Han, J. Zhou, D. Zhou, W. Tang, J. B. Goodenough, Joule 2020, 4, 1864.
- [47] D. T. Boyle, S. C. Kim, S. T. Oyakhire, R. A. Vilá, Z. Huang, P. Sayavong, J. Qin, Z. Bao, Y. Cui, J. Am. Chem. Soc. 2022, 144, 20717.
- [48] X. R. Chen, B. C. Zhao, C. Yan, Q. Zhang, Adv. Mater. 2021, 33, 2004128.
- [49] N. Yao, X. Chen, Z.-H. Fu, Q. Zhang, Chem. Rev. 2022, 122, 10970.
- [50] H. Kang, H. Kang, M. Lyu, E. Cho, EcoMat 2024, 6, 12498.
- [51] P. Li, H. Kim, J. Ming, H.-G. Jung, I. Belharouak, Y.-K. Sun, eScience 2021, 1, 3.
- [52] T. Zheng, Z. Ju, G. Yu, EcoMat 2025, 7, 12518.
- [53] J. Lee, S. H. Jeong, J. S. Nam, M. Sagong, J. Ahn, H. Lim, I. D. Kim, EcoMat 2023, 5, 12416.
- [54] J. P. Wang, F. Lang, Q. Li, EcoMat 2023, 5, 12354.
- [55] B. Wu, C. Chen, L. H. J. Raijmakers, J. Liu, D. L. Danilov, R.-A. Eichel, P. H. L. Notten, Energy Storage Mater. 2023, 57, 508.
- [56] Y. Wang, J. Liang, X. Song, Z. Jin, Energy Storage Mater. 2023, 54, 732.
- [57] W. Li, Z. He, Y. Jie, F. Huang, Y. Chen, Y. Wang, W. Zhang, X. Zhu, R. Cao, S. Jiao, Adv. Funct. Mater. 2024, 34, 2406770.
- [58] Z. Li, Y. Chen, X. Yun, P. Gao, C. Zheng, P. Xiao, Adv. Funct. Mater. 2023, 33, 2300502.
- [59] Z. Wang, H. Wang, S. Qi, D. Wu, J. Huang, X. Li, C. Wang, J. Ma, EcoMat 2022, 4, 12200.
- [60] H. Yang, J. Li, Z. Sun, R. Fang, D.-W. Wang, K. He, H.-M. Cheng, F. Li, Energy Storage Mater. 2020, 30, 113.
- [61] H. Kwon, J. Baek, H.-T. Kim, Energy Storage Mater. 2023, 55, 708.

16146840, 2025, 34, Downloaded from https://advanced.onlinelibrary.wiley.com/doi/10.1002/senm.202502654 by HONG KONG POLYTECHNIC UNIVERSITY HU NG HOM, Wiley Online Library on [25.09/2025]. See the Terms and Conditions (https://onlinelibrary.

onditions) on Wiley Online Library for rules of use; OA articles are governed by the applicable Creative

www.advenergymat.de

- [62] W. Zhou, M. Zhang, X. Kong, W. Huang, Q. Zhang, Adv. Sci. 2021, 8, 2004490.
- [63] Y. Chen, Q. Huang, T. H. Liu, X. Qian, R. Yang, EcoMat 2023, 5, 12385.
- [64] P. Wang, Y. Li, L. Wang, J. Kłos, Z. Peng, N. Kim, H. Bluhm, K. Gaskell, P. Liu, S. B. Lee, B. W. Eichhorn, Y. Wang, *EcoMat* 2020, 2, 12023.
- [65] Y. Yamada, J. Wang, S. Ko, E. Watanabe, A. Yamada, Nat. Energy 2019, 4, 269.
- [66] C. Song, S. H. Han, H. Moon, N. S. Choi, *EcoMat* **2024**, *6*, 12476.
- [67] X. Cao, H. Jia, W. Xu, J.-G. Zhang, J. Electrochem. Soc. 2021, 168, 010522
- [68] W. Liu, J. Li, W. Li, H. Xu, C. Zhang, X. Qiu, Nat. Commun. 2020, 11, 3629.
- [69] A. J. Louli, A. Eldesoky, R. Weber, M. Genovese, M. Coon, J. deGooyer, Z. Deng, R. T. White, J. Lee, T. Rodgers, R. Petibon, S. Hy, S. J. H. Cheng, J. R. Dahn, *Nat. Energy* 2020, 5, 693.
- [70] J. Zhou, X. Lian, Q. Shi, Y. Liu, X. Yang, A. Bachmatiuk, L. Liu, J. Sun, R. Yang, J.-H. Choi, M. H. Rummeli, Adv. Energy Sustainability Res. 2021, 3, 2100140.
- [71] Z. Zeng, V. Murugesan, K. S. Han, X. Jiang, Y. Cao, L. Xiao, X. Ai, H. Yang, J.-G. Zhang, M. L. Sushko, J. Liu, Nat. Energy 2018, 3, 674.
- [72] Z. Wang, R. Han, H. Zhang, D. Huang, F. Zhang, D. Fu, Y. Liu, Y. Wei, H. Song, Y. Shen, J. Xu, J. Zheng, X. Wu, H. Li, Adv. Funct. Mater. 2023, 33, 2215065.
- [73] Z. Cui, Z. Jia, D. Ruan, Q. Nian, J. Fan, S. Chen, Z. He, D. Wang, J. Jiang, J. Ma, X. Ou, S. Jiao, Q. Wang, X. Ren, *Nat. Commun.* 2024, 15, 2033.
- [74] Z. Wang, Y. Sun, Y. Mao, F. Zhang, L. Zheng, D. Fu, Y. Shen, J. Hu, H. Dong, J. Xu, X. Wu, Energy Storage Mater. 2020, 30, 228.
- [75] H. Dinh Nguyen, T. Duong Pham, A. Bin Faheem, H. Min Oh, K. K. Lee, Batteries Supercaps 2022, 6, 202200453.
- [76] X. Zhang, L. Zou, Y. Xu, X. Cao, M. H. Engelhard, B. E. Matthews, L. Zhong, H. Wu, H. Jia, X. Ren, P. Gao, Z. Chen, Y. Qin, C. Kompella, B. W. Arey, J. Li, D. Wang, C. Wang, J. G. Zhang, W. Xu, Adv. Energy Mater. 2020, 10, 2000368.
- [77] S. Ko, Y. Yamada, A. Yamada, Batteries Supercaps 2020, 3, 910.
- [78] J. Holoubek, M. Yu, S. Yu, M. Li, Z. Wu, D. Xia, P. Bhaladhare, M. S. Gonzalez, T. A. Pascal, P. Liu, Z. Chen, ACS Energy Lett. 2020, 5, 1438
- [79] S. Zhang, S. Li, X. Wang, C. Li, Y. Liu, H. Cheng, S. Mao, Q. Wu, Z. Shen, J. Mao, H. Pan, Y. Lu, Nano Energy 2023, 114, 108639.
- [80] C.-C. Su, M. He, M. Cai, J. Shi, R. Amine, N. D. Rago, J. Guo, T. Rojas, A. T. Ngo, K. Amine, *Nano Energy* **2022**, *92*, 106720.
- [81] L. L. Jiang, C. Yan, Y. X. Yao, W. Cai, J. Q. Huang, Q. Zhang, Angew. Chem., Int. Ed. 2020, 60, 3402.
- [82] Z. Yu, P. E. Rudnicki, Z. Zhang, Z. Huang, H. Celik, S. T. Oyakhire, Y. Chen, X. Kong, S. C. Kim, X. Xiao, H. Wang, Y. Zheng, G. A. Kamat, M. S. Kim, S. F. Bent, J. Qin, Y. Cui, Z. Bao, Nat. Energy 2022, 7, 94.
- [83] J. Zhou, C. Zhang, H. Wang, Y. Guo, C. Xie, Y. Luo, C. Wang, S. Wen, J. Cai, W. Yu, F. Chen, Y. Zhang, Q. Huang, Z. Zheng, Adv. Sci. 2024, 11, 2410129.
- [84] S. Ko, Y. Yamada, A. Yamada, Joule 2021, 5, 998.
- [85] X. Ren, P. Gao, L. Zou, S. Jiao, X. Cao, X. Zhang, H. Jia, M. H. Engelhard, B. E. Matthews, H. Wu, H. Lee, C. Niu, C. Wang, B. W. Arey, J. Xiao, J. Liu, J.-G. Zhang, W. Xu, Proc. Natl. Acad. Sci. USA 2020, 117, 28603.
- [86] X. Cao, P. Gao, X. Ren, L. Zou, M. H. Engelhard, B. E. Matthews, J. Hu, C. Niu, D. Liu, B. W. Arey, C. Wang, J. Xiao, J. Liu, W. Xu, J.-G. Zhang, Proc. Natl. Acad. Sci. USA 2021, 118, 2020357118.

- [87] X. Cao, L. Zou, B. E. Matthews, L. Zhang, X. He, X. Ren, M. H. Engelhard, S. D. Burton, P. Z. El-Khoury, H.-S. Lim, C. Niu, H. Lee, C. Wang, B. W. Arey, C. Wang, J. Xiao, J. Liu, W. Xu, J.-G. Zhang, Energy Storage Mater. 2021, 34, 76.
- [88] G. Xu, X. Shangguan, S. Dong, X. Zhou, G. Cui, Angew. Chem., Int. Ed. 2019, 59, 3400.
- [89] J. Wang, Y. Yamada, K. Sodeyama, C. H. Chiang, Y. Tateyama, A. Yamada, Nat. Commun. 2016, 7, 12032.
- [90] Y. Wang, Z. Wu, F. M. Azad, Y. Zhu, L. Wang, C. J. Hawker, A. K. Whittaker, M. Forsyth, C. Zhang, Nat. Rev. Mater. 2023, 9, 119.
- [91] M. Mao, X. Ji, Q. Wang, Z. Lin, M. Li, T. Liu, C. Wang, Y.-S. Hu, H. Li, X. Huang, L. Chen, L. Suo, Nat. Commun. 2023, 14, 1082.
- [92] I. R. Choi, Y. Chen, A. Shah, J. Florian, C. Serrao, J. Holoubek, H. Lyu, E. Zhang, J. H. Lee, Y. Lin, S. C. Kim, H. Park, P. Zhang, J. Lee, J. Qin, Y. Cui, Z. Bao, Nat. Energy 2025, 10, 365.
- [93] X. Wang, M. Salari, D.-e. Jiang, J. C. Varela, B. Anasori, D. J. Wesolowski, S. Dai, M. W. Grinstaff, Y. Gogotsi, Nat. Rev. Mater. 2020, 5, 787.
- [94] H. Sun, G. Zhu, Y. Zhu, M. C. Lin, H. Chen, Y. Y. Li, W. H. Hung, B. Zhou, X. Wang, Y. Bai, M. Gu, C. L. Huang, H. C. Tai, X. Xu, M. Angell, J. J. Shyue, H. Dai, Adv. Mater. 2020, 32, 2001741.
- [95] C. Weng, L. Ma, B. Wang, F. Meng, J. Yang, Y. Ji, B. Liu, W. Mai, S. Huang, L. Pan, J. Li, Energy Storage Mater. 2024, 71, 103584.
- [96] S. Lee, K. Park, B. Koo, C. Park, M. Jang, H. Lee, H. Lee, Adv. Funct. Mater. 2020, 30, 2003132.
- [97] J. Jang, C. Wang, G. Kang, C. Han, J. Han, J.-S. Shin, S. Ko, G. Kim, J. Baek, H.-T. Kim, H. Lee, C. B. Park, D.-H. Seo, Y. Li, J. Kang, *Nat. Energy* 2025, 10, 502.
- [98] Z. Wang, F. Zhang, Y. Sun, L. Zheng, Y. Shen, D. Fu, W. Li, A. Pan, L. Wang, J. Xu, J. Hu, X. Wu, Adv. Energy Mater. 2021, 11, 2003752
- [99] Z. Wang, H. Zhang, J. Xu, A. Pan, F. Zhang, L. Wang, R. Han, J. Hu, M. Liu, X. Wu, Adv. Funct. Mater. 2022, 32, 2112598.
- [100] Y. Li, F. Ding, Y. Shao, H. Wang, X. Guo, C. Liu, X. Sui, G. Sun, J. Zhou, Z. Wang, Angew. Chem., Int. Ed. 2024, 63, 202317148.
- [101] F. Ding, Y. Li, G. Zhang, H. Wang, B. Liu, C. Liu, L. Jiang, X. Sui, Z. Wang, Adv. Mater. 2024, 36, 2400177.
- [102] W. Zou, J. Zhang, M. Liu, J. Li, Z. Ren, W. Zhao, Y. Zhang, Y. Shen, Y. Tang, Adv. Mater. 2024, 36, 2400537.
- [103] C. Zuo, D. Dong, H. Wang, Y. Sun, Y.-C. Lu, Energy Environ. Sci. 2024, 17, 791.
- [104] J. He, A. Bhargav, L. Su, J. Lamb, J. Okasinski, W. Shin, A. Manthiram, Nat. Energy 2024, 9, 446.
- [105] S. Chen, J. Zheng, L. Yu, X. Ren, M. H. Engelhard, C. Niu, H. Lee, W. Xu, J. Xiao, J. Liu, J.-G. Zhang, *Joule* 2018, 2, 1548.
- [106] X. Wang, W. He, H. Xue, D. Zhang, J. Wang, L. Wang, J. Li, Sustainable Energy Fuels 2022, 6, 1281.
- [107] Q. Zheng, Y. Yamada, R. Shang, S. Ko, Y.-Y. Lee, K. Kim, E. Nakamura, A. Yamada, *Nat. Energy* **2020**, *5*, 291.
- [108] C. Zhang, S. Gu, D. Zhang, J. Ma, H. Zheng, M. Zheng, R. Lv, K. Yu, J. Wu, X. Wang, Q.-H. Yang, F. Kang, W. Lv, Energy Storage Mater. 2022, 52, 355.
- [109] Z. Xu, X. Zhang, J. Yang, X. Cui, Y. Nuli, J. Wang, Nat. Commun. 2024, 15, 9856.
- [110] J. Wang, Y. Yamada, K. Sodeyama, E. Watanabe, K. Takada, Y. Tateyama, A. Yamada, Nat. Energy 2017, 3, 22.
- [111] L. Tan, S. Chen, Y. Chen, J. Fan, D. Ruan, Q. Nian, L. Chen, S. Jiao, X. Ren, Angew. Chem., Int. Ed. 2022, 61, 202203693.

www.advenergymat.de

16 14684, 2023, 34, Downloaded from https://advanced.onlinelibrary.wiley.com/doi/10.1002/amm.20259254 by HONG KONG POLYTECHNIC UNIVERSITY HU NG HOM, Wiley Online Library on [25.69)2025]. See the Terms and Conditions (https://onlinelibrary.wiley.com/terms-ad-conditions) on Wiley Online Library for rules of use; OA arctics as agreement by the applicable Clerity Commons



Junhua Zhou is currently Research Assistant Professor at the Department of Applied Biology and Chemical Technology (ABCT), The Hong Kong Polytechnic University (PolyU). He received his Ph.D. (2022) in Materials Science and Engineering from the Soochow University. After a postdoctoral stay in Prof. Zijian Zheng's group, he joined the ABCT at PolyU as a Research Assistant Professor in 2025. His research interests mainly include high-voltage lithium metal battery, lithium sulfur battery, solid-state battery, and advanced characterization techniques.



Huimin Wang received her Ph.D. in Energy Storage Materials and Science from the City University of Hong Kong. She is currently a Postdoctoral Fellow at the Department of Applied Biology and Chemical Technology, The Hong Kong Polytechnic University. Her research focuses on advanced energy storage materials and devices, with an emphasis on high-performance and multifunctional electrolyte design for next-generation energy storage systems.



Yongqiang Yang received his B.S. degree in School of Minerals Processing and Bioengineering (2016), and M.Eng. (2019), Ph.D. (2023) degrees in School of Materials Science and Engineering at the Central South University. Currently, he is a RGC Postdoctoral Fellow in Department of Applied Biology and Chemical Technology at The Hong Kong Polytechnic University. His research interests focus on Znbased batteries and halogen redox chemistry.



Can Guo received her Ph.D. degree under the supervision of Prof. Ya-Qian Lan and Prof. Yifa Chen from the South China Normal University in 2024. She is currently a Postdoctoral Fellow at the Hong Kong Polytechnic University with Prof. Zijian Zheng. Her research focuses on the design and construction of crystalline porous materials and their applications in battery.



16146840, 2025, 34, Downloaded from https://advanced.onlinelibrary.wiley.com/doi/10.1002/senm.202502654 by HONG KONG POL YTECHNIC UNIVERSITY HU NG HOM, Wiley Online Library on [25.09/2025]. See the Terms

and Conditions (https://onlinelibrary.wiley.com/terms-and-conditions) on Wiley Online Library for rules of use; OA articles are governed by the applicable Creative



Zhibo Li received his B.Eng. degree from the South China Normal University in 2018 and M.S. degree from the Peking University in 2021. Now he is a Ph.D. candidate in The Hong Kong Polytechnic University. His research interests mainly focus on solid-state batteries and lithium metal batteries.



Zhaokun Wang received his bachelor's degree in Microelectronics Science and Engineering from the Southern University of Science and Technology and master's degree in Materials Science and Engineering from the University of California, Irvine, CA. Now he is a Ph.D. candidate in The Hong Kong Polytechnic University. His research interests mainly focus on lithium metal batteries, interfacial engineering, and electron microscopy.



Yufei Zhang is currently a Research Assistant Professor in the Department of Applied Biology and Chemical Technology, The Hong Kong Polytechnic University. She received her Ph.D. degree in Textile Science and Engineering from the Donghua University in 2021, under the supervision of Prof. Bin Ding and Prof. Xianfeng Wang. She joined The Hong Kong Polytechnic University as a Postdoctoral Fellow in 2022, working with Chair Prof. Zijian Zheng. Her research interests include soft electronics and smart wearables, thermal and moisture managing electronic textiles, biomimetic nanofibrous materials, and supramolecular polymers.



Qiyao Huang is currently Assistant Professor at School of Fashion & Textiles, The Hong Kong Polytechnic University. She received her B.A. in Fashion and Textiles (2014) and Ph.D. (2019) in Textile Technology from The Hong Kong Polytechnic University. After a postdoctoral stay in Prof. Zijian Zheng's group, she joined the Institute of Textiles and Clothing at The Hong Kong Polytechnic University as a Research Assistant Professor in 2020. Her research interests include conductive textiles, flexible and stretchable electrodes, and textile-based devices for electrochemical energy storage and sensing applications.

www.advenergymat.de



16146840, 2023, 34, Downloaded from https://advanced.onlinelibrary.wiley.com/doi/10.1002/aenm.202302654 by HONG KONG POLYTECHNIC UNIVERSITY HU NG HOM, Wiley Online Library on [250/92025]. See the Terms



Zijian Zheng earned his B.Eng. in Chemical Engineering from Tsinghua University (2003) and his Ph.D. in Chemistry from the University of Cambridge (2007). He is now Chair Professor in The Hong Kong Polytechnic University and Associate Director of both the Research Institute of Wearable Intelligent Systems and Research Facility in Materials Characterization and Device Fabrication. His research spans surface science, nanofabrication, flexible electronics, and energy. He serves as Editor-in-Chief of EcoMat and holds editorial roles with several leading journals. His honors include Founding Member of the Hong Kong Young Academy of Sciences and Chang Jiang Chair Professor.